Chemical Papers
https://doi.org/10.1007/s11696-021-01730-8

ORIGINAL PAPER

Design, synthesis and biological evaluation of some novel N'-(1,3-benzothiazol-2-yl)-arylamide derivatives as antibacterial agents

Swarupa Rani Gurram[1] · **Mohammed Afzal Azam**[1]

Received: 13 February 2021 / Accepted: 5 June 2021

Abstract

In the present work, we carried out hydroxybenzotriazole (HOBT) and 1-(3-dimethylaminopropyl)-3-ethylcarbodiimide hydrochloride (EDCl)-mediated synthesis of new N'-(1,3-benzothiazol-2-yl)-arylamides $C_{1\text{-}18}$ in high yields under relatively milder reaction conditions using dimethyl formamide as solvent. Synthesized compounds were characterized by FTIR, ^{1}H-NMR, ^{13}C-NMR and HRMS spectral data. The MIC values of synthesized compounds $C_{1\text{-}18}$ were determined by the broth microdilution method using Mueller Hinton medium. Tested compounds showed variable activity against the tested Gram-positive and Gram-negative bacterial strains. Compounds C_3, C_5, C_9, $C_{13\text{-}15}$ and C_{17} exhibited promising activity against *Staphylococcus aureus* NCIM 5021 with MIC values in the range of 19.7–24.2 µM. Among all tested compounds, C_{13} possessing thiophene ring attached to the benzothiazole moiety via amide linkage exhibited maximum activity against *S. aureus* NCIM 5022 with MIC of 13.0 µM. Compound C_{13} showed maximum activity against *S. aureus* ATCC 43300 with MIC of 15.0 µM and exhibited bactericidal activity against this strain in minimum bactericidal concentration determination. This compound also eliminated *S. aureus* ATCC 43300 strain after 24-h exposure indicating its bactericidal activity. ADMET calculation showed favourable pharmacokinetic profile of synthesized compounds $C_{1\text{-}18}$.

Graphic abstract

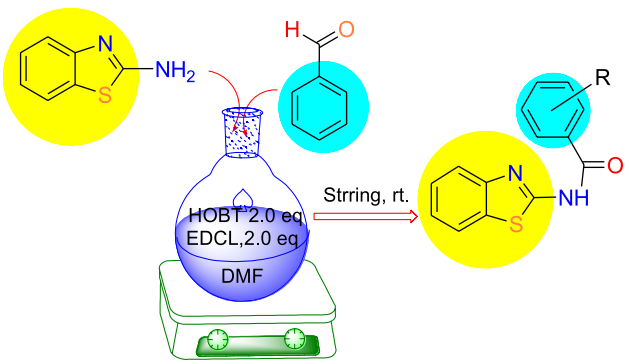

Keywords N'-(1,3-benzothiazol-2-yl)-arylamides · HOBt/EDCl · MIC · MBC · Time-kill study

Introduction

Benzothiazole (BT) is a privileged bicyclic heterocyclic moiety present in a wide variety of synthetic and natural products. BT derivatives are manufactured worldwide for a wide variety of applications (Azam and Suresh 2012). BT derivatives act as important scaffold and played an important

✉ Mohammed Afzal Azam
afzal9azam@hotmail.com; afzal@jssuni.edu.in

[1] Department of Pharmaceutical Chemistry, JSS College of Pharmacy, Tamil Nadu (JSS Academy of Higher Education and Research), Ooty, Nilgiris 643001, India

Published online: 14 June 2021

role in the field of medicinal chemistry. BTs have been investigated extensively and associated with diverse biological activities such as antifungal (Catalano et al. 2013), antiprotozoal (Delmas et al. 2002), antimicrobial (Amnerkar and Bhusari 2011), anticancer (Cai et al. 2013; Cindric et al. 2018), anticonvulsant (Liu et al. 2016), antihypertensive (Meltzer-Mats et al. 2013), antidiabetic (Mariappan et al. 2012), anti-inflammatory (Ugwu et al. 2018) activities. 2-Aminobenzothiazoles are also investigated for their larvicidal and adulticidal activities against *Aedes aeaegypti* (Sever et al. 2019).

Several drugs are also available in the market containing benzothiazole nucleus, including glutamate transporter inducer riluzole (Zoccolella et al. 2007) intended for the treatment of amyotrophic lateral sclerosis, carbonic anhydrase 1–4 and 7 inhibitor ethoxzolamide (Heck et al. 1994) indicated for the treatment of glaucoma and as a diuretic, mast cell stabilizer Tiaramide (Berkin and Kerr 1982) used as an antiasthmatic drug, Dopamine D2–D4 receptor receptor agonist Pramipexole (Mierau et al. 1995) used to treat Parkinson's disease, dual D2 dopamine receptor and β2-adrenoceptor agonist Sibenadet (Laursen et al. 2003) for alleviating the symptoms of chronic obstructive pulmonary disease, Frentizole an inhibitor of the Aβ-ABAD interaction used as an immunosuppressive agent (Xie et al., 2006). In addition, Phortress (Bradshaw and Westwell 2004) is in clinical trials for the treatment of solid tumour (formation of extensive DNA adducts). Many patents have been published on benzothiazole derivatives highlighting its importance, and few derivatives are in different phases of clinical trials (Svendsen et al. 2021; Waynne et al., 2009; Klunk et al. 2014; Dahl et al. 2015; Sutton et al. 2009). Further, N-benzothiazol-2-yl-amides have been shown to be associated with wide range of biological activities such as inhibition of ubiquitin ligase (Parlati et al. 2005), selective cytotoxicity against tumorigenic cell lines (Yoshida et al. 2005), prophylaxis and treatment of rotavirus infections (Bailey and Pevear 2004), the adenosine A_{2A} receptor modulators (Alanine et al. 2001) and therapeutic agents for disorders associated with nuclear hormone receptors (Kerwin et al. 1997). In particular, some benzothiazoles substituted at the second position with a substituted benzoylamino moiety showed activity against *Brugia malayi* thymidylate kinase (Sashidhara et al. 2015) and *Mycobacterium tuberculosis* H37Rv strain (Hazra et al. 2012). The amide functionality is known to be important functional group due to its presence in nature and chemical industry, biomolecules and medicinal agents (Greenberg 2000).

High-throughput screening campaign by Franzblau et al. (2012) identified unsubstituted benzothiazole adamantly amide 1 (Fig. 1) with promising activity against *Mycobacteroides abscessus* (MIC, 1 µg/mL). This compound was further optimized by Graham et al. (2018) to overcome its high lipophilicity and potential for nonspecific binding. Replacement of the adamantyl group with methyl-substituted cyclohexyl and substitution of trifluoromethyl group at position five of benzothiazole ring resulted in compound **2** with potent activity against *M. tuberculosis* H37Rv (MIC, $\leq$0.12 µg/mL). Further, replacement of the adamantyl group with 1-methylbicyclo[3.3.1]nonane ring and substitution of 5-Br-/5,7-dichloro-/4,5,6-trifluoro-2-aminobenzothiazole amide groups (compounds 3, 4 and 5, respectively) in place of 2-aminobenzothiazole amide resulted in potent and specific activity against *M. tuberculosis* H37Rv (MIC of $\leq$0.12 µg/mL in all three cases). However, compounds 2–6 exhibited lower activity against *Mycobacterium avium* 101 and *Mycobacteroides abscessus* 19,977 (MICs, 1.0 to > 64 µg/mL). Further, replacement of 5-trifluoromethyl-2-aminobenzothiazole ring in compound 2 by 4,6-difluoro-2-amino benzothiazol resulted in compound 6 with potent activity against *M. tuberculosis* H37Rv (MIC of $\leq$0.12 µg/mL). Replacement of 5-Br-/5,7-dichloro-/4,5,6-trifluoro-2-aminobenzothiazoles in compounds 3–5 by 5,7-dichloro and 7-trifluoromethoxy-2-aminobenzothiazoles resulted, respectively, in compounds 7 and 8 (De Groote et al. 2018). These two compounds were observed to be significantly active against the tested rapid growing non-tuberculous mycobacteria (MICs, 0.03 to $\leq$0.06 µg/mL). However, these two compounds showed poor or less activity (MICs, 8 to > 64 µg/mL) against tested strains of both Gram-positive and Gram-negative bacteria *Staphylococcus aureus* ATCC 29213, *Enterococcus faecalis* ATCC 29212, *Streptococcus pyogenes* ATCC 19615, *Streptococcus pneumoniae* ATCC 49619, *Escherichia coli tolC* CGSC 5633 and *Pseudomonas aeruginosa* ATCC 35151. It is evident from the above result that the substitution of halogen atoms or halo-containing groups imparted specific activity either against *M. tuberculosis* or non-tuberculous mycobacteria. Benzothiazole-bearing amide 9 (Fig. 1) also displayed promising activity against *S. aureus* ATCC 25323 (MIC, 15.6 µg/mL), *E. coli* ATCC 35218 (MIC, 7.81 µg/mL) and *K. pneumonia* ATCC 31488 (MIC, 3.91 µg/mL) (Bhat et al. 2017). In another attempt, Patel et al. (2012) identified benzothiazole acetamide derivative (compound 10 Fig. 1), with significant antibacterial activity against *Staphylococcus aureus* (MIC, 3.12 µg/mL), *Bacillus cereus* (MIC, 6.25 µg/mL) and *Shigella flexneri* MIC, 6.25 µg/mL). Benzothiazole derivatives 11 possessing acetamide function have been synthesized and evaluated for their antimicrobial activity (Srivastava and Sen 2008). Some of the compounds also exhibited promising activity against *S. aureus*, *E. coli*, *K. pneumoniae* and *Bacillus subtilis*.

Molecular hybridization is known medicinal chemistry strategy used to combine two different scaffolds into a single chemical entity. It is a well-known approach employed for the design of ligands to increase the affinity towards targets

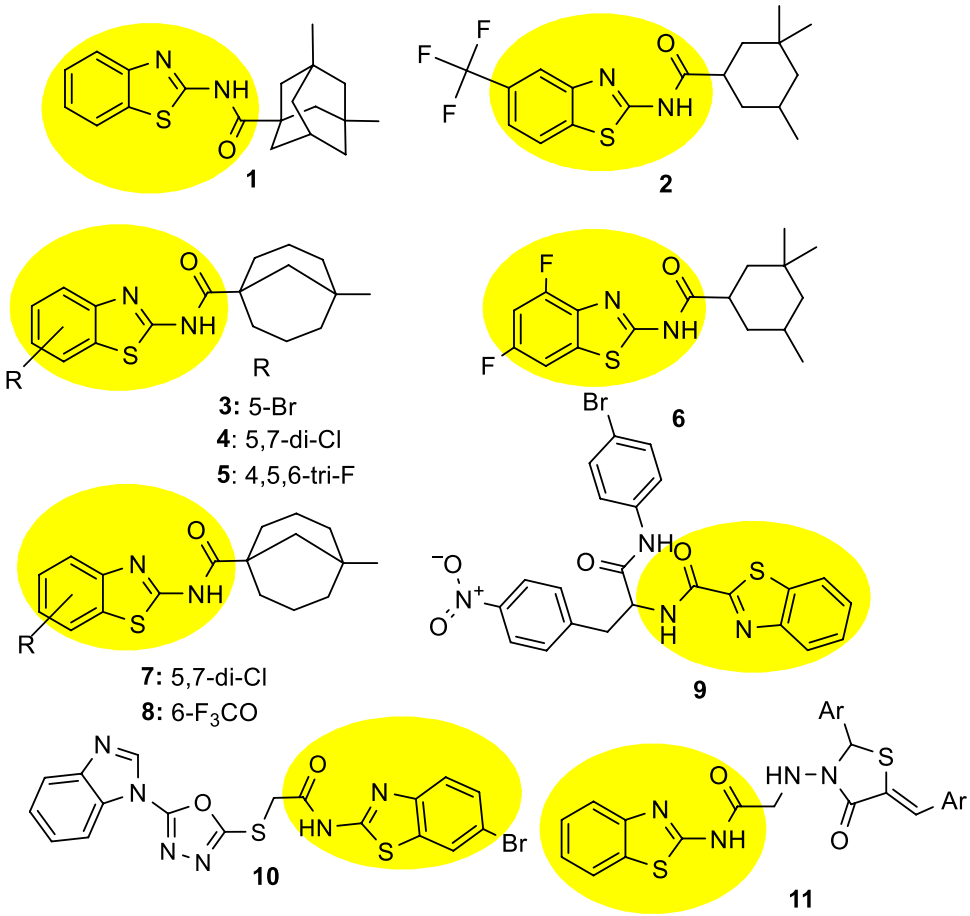

Fig. 1 Design concept of title compounds $C_{1\text{-}18}$

of interest (Makhaeva et al. 2020; Gontijo et al. 2020). Based on these observations, we sought to combine unsubstituted benzothiazole ring with alkyl/aryl hydrazide moieties in a single molecular scaffold in an attempt to develop broad-spectrum antibacterial agents.

Amidation reaction is among the most used transformations in medicinal and organic chemistry. Although *N*-acyl 2-aminobenzothiazoles play an important role in medicinal chemistry, the available synthetic strategies that lead to these compounds are limited (Santos et al. 2020). These molecules have been synthesized by the N-heterocyclic carbene (NHC) organocatalysed direct oxidative amidation of araldehydes with 2-aminobenzothiazoles in dichloromethane using triazolium salt as carbine precursor and Cs_2CO_3 as base (Premaletha et al. 2017). These compounds showed diverse biological activities like anti-infective, inhibitors of protein–protein interaction, inhibitor of nuclear hormone receptors, anticonvulsant, antitubercular and anticancer. Direct coupling of 2-aminobenzothiazole with acid chlorides in glacial acetic acid has yielded N-benzothiazol-2-yl-amides in 55–80% yield (Saraswat et al. 2018). Coupling of 2-aminobenzothiazole with different acid chlorides using dimethylformamide and triethylamine has also been applied (Cindric et al. 2018). N-benzothiazol-2-yl-amide was also prepared by coupling of 2-amin-4-nitrobenzothiazole and acid chloride using Eaton's reagent under microwave. Several other approaches (Shaik et al. 2019; Wang et al. 2017; Castanheiro et al. 2016; Kim et al. 2013) have also been used for the synthesis of N-benzothiazol-2-yl-amide. In the present work, we designed eighteen molecules $C_{1\text{-}18}$ by linking benzothiazole nucleus with substituted aryl/aralkyl pharmacophores via amide linkage. All these molecules were synthesized in high yields by direct coupling of 2-aminobenzothiazole (A) with carboxylic acids ($B_{1\text{-}18}$) under the catalysis of 1-hydroxybenzotriazole (HOBt) and 1-ethyl-3-(3-dimethylaminopropyl) carbodiimide hydrochloride (EDCl) and subsequently evaluated for their antibacterial activity against selected strains of bacteria.

Experimental

Material and methods

All glass wares were oven-dried prior to use. The purification and drying of solvents were carried wherever required. All reactions were examined by thin-layer chromatography (TLC) using pre-coated aluminium back thin layer

chromatography (TLC) silica gel F_{254} plates (Merck Ltd., Germany). Chemicals and solvents were purchased from Sigma-Aldrich, Merck, Alfa Aesar, Finar Pvt. Ltd., India, and LOBA Chemie Pvt., Ltd. India. The melting point of the synthesized compounds was determined using Veego VMP-1 melting point apparatus expressed in °C and is uncorrected. Fourier transform infrared (FT-IR) spectra were recorded either with Shimadzu 8400 s or with PerkinElmer-Spectrum Two spectrometers. ^{1}H and ^{13}C-NMR spectra were recorded either in deuterated chloroform ($CDCl_3$) or in dimethyl sulphoxide (DMSO-d_6) at 300–500 and 100 MHz, respectively, using Bruker AV-III 400 spectrometer (Germany). Chemical shifts were recorded in ppm using the solvent as internal standard. The peak patterns are given as s, singlet; d, doublet; t, triplet; td, triple doublet; dd, doublet of doublets; m, multiplet. High-resolution mass spectra (HRMS) were measured using Xevo G2-XS QT of Quadrupole Time-of-Flight Mass Spectrometer (USA) with positive electrospray ionization (ESI) mode at 70 eV, as shown in Table 1.

General procedure for the synthesis of N′-(1,3-benzothiazol-2-yl)-4-substituted benzamides ($C_{1\text{-}18}$)

1,3-Benzothiazole-2-amine (A) (0.242 g, 0.0014 mol) and HOBt (0.450 g, 0.0029 mol) were successively added to the corresponding aromatic acids ($B_{1\text{-}18}$) (0.2 g, 0.0014 mol) dissolved in N,N-dimethylformamide (DMF) (15 mL). The mixture was cooled to 0 °C in an ice bath with stirring, and then, EDCl (0.563 g, 0.00294 mol) was added. The reaction mixture was then slowly allowed to reach the room temperature over 1 h, and then, stirring was further continued at this temperature till completion of reaction. Progress of reaction was monitored with TLC using n-hexane:ethylacetate (1:2 to 1:6) as eluent. The reaction was quenched by adding saturated $NaHCO_3$ solution and then extracted with ethylacetate (20 mL × 3). The organic layer was dried with anhydrous Na_2SO_4, filtered and concentrated under reduced pressure. The residue thus obtained was purified by column chromatography on silica gel Merck (200 mesh) in glass columns (2 or 3 cm diameter) using 25–30 g of silica gel per one gram of the residue. The elution of column was started with n-hexane, and then, eluent polarity was gradually increased with ethyl acetate. Compounds $C_{1\text{-}18}$ thus obtained in the yield of 80–95%.

Synthetic route and chemical structures of compounds $C_{1\text{-}18}$ are presented, respectively, in Scheme 1 and Table 2.

Table 1 Optimization of reaction conditions in the model reaction

Entry	Solvent	HOBt/EDCl	Temperature (°C)	Time	Yield (%)[a]
1	CH_3CN	2.0 equivalent each	25	18	25.3
2	CH_3COCH_3	2.0 equivalent each	25	24	30.2
3	$CHCl_3$	2.0 equivalent each	25	24	30.1
4	CH_2Cl_2	2.0 equivalent each	25	24	18.6
5	THF	2.0 equivalent each	25	24	29.2
6	DMF	2.0 equivalent each	25	12	85.6
7	DMF	1.5 equivalent each	25	24	32.1

[a]Isolated yield

N-(1,3-benzothiazol-2-yl)-2-fluorobenzamide (C_1)

White solid; yield: 85.6%. M.P: 170–172 °C. *Rf* = 0.66 (ethylacetate/n-hexane, V/V = 3:7). FT-IR (cm^{-1}): 3260 (NH), 3021 (Ar C–H), 1656 (> C=O), 1623 (> C=N), 1595, 1566 (Ar –C=C–), 1518 (amide II), 767 (ortho-substituted benzene), 671 (C–S–C). ^{1}H-NMR (300 MHz, DMSO-d_6) δ_{ppm} 12.81 (s, 1H, NH), 7.99 (d, *J* = 7.7 Hz, 1H), 7.76 (dd, *J*FH3′H4′ = 91.45 Hz, 2H), 7.61 (td, *J*FH5′ = 73.17, Hz, 1H), 7.39–7.46 (m, 1H), 7.25–7.38 (m, 3H). ^{13}C-NMR (100 MHz, $CDCl_3$) δ_{ppm} 161.69 (> C=O), 160.96 (> C=N), 159.21, 157.36, 148.02, 134.91, 134.81, 131.94, 125.98, 125.01, 123.78, 121.04, 120.68, 118.68, 118.58, 116.31, 116.07. ^{19}F-NMR (377 MHz, DMSO-d_6): δ_{ppm} 113.27. HRMS (ESI-TOF) (m/z): $[M+H]^+$ Calcd. for: $C_{14}H_{10}N_2OSF$ 273.0498; Found 273.0489.

N-(1,3-benzothiazol-2-yl)-4-methylbenzamide (C_2).

White powder; yield: 80.5%. M.P: 160–162 °C. *Rf* = 0.65 (ethylacetate/n-hexane, V/V = 2:8). FT-IR (cm^{-1}): 3285 (NH), 3013 (Ar C–H), 1663 (> C=O), 1618 (> C=N), 1592, 1542 (Ar –C=C–), 1525 (amide II), 821 (para-substituted benzene), 669 (C–S–C). ^{1}H-NMR (300 MHz, $CDCl_3$) δ_{ppm} 8.18 (d, *J* = 8.2 Hz, 2H), 8.11 (d, *J* = 8.3 Hz, 1H), 7.62–7.52 (m, 1H),

Scheme 1 Route for the synthesis of tilted compounds $C_{1\text{-}18}$

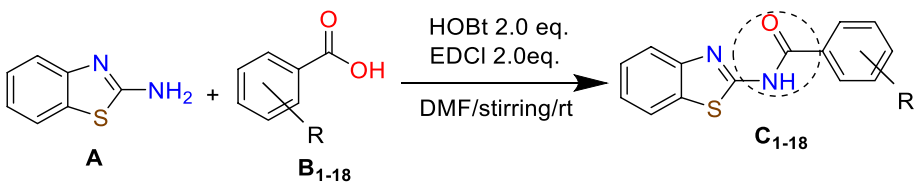

Table 2 Chemical structures of the synthesized compounds $C_{1\text{-}18}$

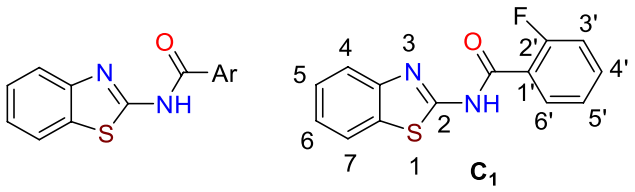

C_1

Comp	Ar	Comp	Ar	Comp	Ar
C_1	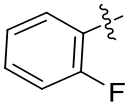	C_7	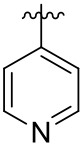	C_{13}	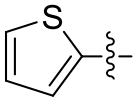
C_2	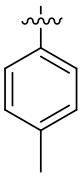	C_8	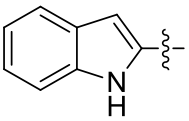	C_{14}	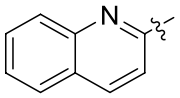
C_3	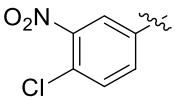	C_9	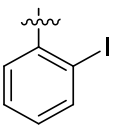	C_{15}	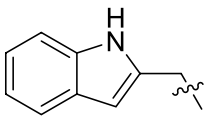
C_4	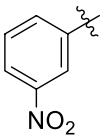	C_{10}	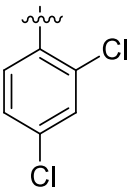	C_{16}	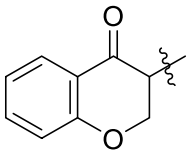
C_5	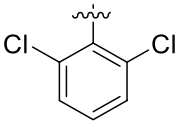	C_{11}	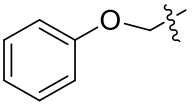	C_{17}	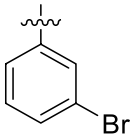
C_6	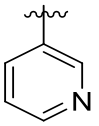	C_{12}	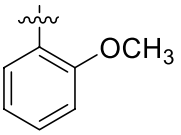	C_{18}	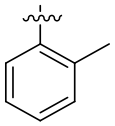

7.47 (dd, $J = 8.2$, 3.9 Hz, 2H), 7.41 (d, $J = 8.1$ Hz, 2H), 2.51 (s, 3H). ^{13}C-NMR (100 MHz, $CDCl_3$) δ_{ppm} 162.81, 146.91, 143.62, 130.86, 129.98, 129.23, 128.89, 128.75, 124.86, 121.97, 120.60, 108.44, 22.06. HRMS (ESI-TOF) (m/z): $[M+H]^+$ Calcd. for: $C_{15}H_{13}N_2OS$ 269.0749; Found 269.0736.

N-(1,3-benzothiazol-2-yl)-4-chloro-3-nitrobenzamide (C_3).

White powder; yield: 86.5%. M.P: 254–256 °C. *Rf* = 0.76 (ethylacetate/n-hexane, V/V = 3:7). FT-IR (cm^{-1}): 3249 (NH), 3025 (Ar C–H), 1648 (> C=O), 1622 (> C=N), 1589, 1567 (Ar –C=C–), 1512 (amide II), 1345, 1545 (NO_2), 665 (C–S–C). ^{1}H-NMR (500 MHz, $CDCl_3$) δ_{ppm} 8.57 (d, $J = 2.1$ Hz, 1H), 8.17 (dd, $J = 8.4$, 2.1 Hz, 1H), 7.86 (d, $J = 7.8$ Hz, 1H), 7.71 (d, $J = 8.4$ Hz, 1H), 7.65 (d, $J = 8.1$ Hz, 1H), 7.48–7.44 (m, 1H), 7.39–7.35 (m, 1H). ^{13}C-NMR (100 MHz, DMSO-d_6) δ_{ppm} 139.67, 125.18, 125.09, 124.19, 123.30, 122.69, 118.28, 118.00, 115.93, 113.56, 111.58. HRMS (ESI-TOF) (m/z): $[M+H]^+$ Calcd. for: $C_{14}H_9ClN_3O_3S$ 334.0047; Found 334.0042.

N-(1,3-benzothiazol-2-yl)-3-nitrobenzamide (C_4).

Pale yellow solid; yield: 84.3%. M.P: 240–242 °C. *Rf* = 0.68 (ethylacetate/n-hexane, V/V = 3:7). FT-IR (cm^{-1}): 3288 (NH), 3011 (Ar C–H), 1659 (> C=O), 1622 (> C=N), 1590, 1577 (Ar –C=C–), 1517 (amide II), 1355, 1547 (NO_2), 672 (C–S–C). ^{1}H-NMR (400 MHz, $CDCl_3$) δ_{ppm} 11.03 (s, 1H, NH), 8.84 (s, 1H), 8.44 (dd, *J* = 8.2, 1.1 Hz, 1H), 8.36 (d, *J* = 7.8 Hz, 1H), 7.93–7.85 (m, 1H), 7.71 (t, *J* = 8.0 Hz, 1H), 7.55 (d, *J* = 7.5 Hz, 1H), 7.43–7.31 (m, 2H). ^{13}C-NMR (100 MHz, DMSO-d_6) δ 163.80, 158.90, 146.76, 145.63, 133.24, 130.07, 128.45, 125.41, 124.81, 122.47, 122.32, 120.09, 118.47. HRMS (ESI-TOF) (m/z): $[M+H]^+$ Calcd. for: $C_{14}H_{10}N_3O_3S$ 300.0437; Found 300.0434.

N-(1,3-benzothiazol-2-yl)-2,6-dichlorobenzamide (C_5).

White powder; yield: 81.3%. M.P: 208–210 °C. *Rf* = 0.56 (ethylacetate/n-hexane, V/V = 3:7). FT-IR (cm^{-1}): 3297 (NH), 3032 (Ar C–H), 1661 (> C=O), 1612 (> C=N), 1593, 1561 (Ar –C=C–), 1530 (amide II), 675 (C-S-C). ^{1}H-NMR (500 MHz, $CDCl_3$) δ_{ppm} 8.57 (d, *J* = 8.4 Hz, 1H), 8.04 (d, *J* = 8.4 Hz, 1H), 7.89 (t, *J* = 7.8 Hz, 1H), 7.66 (t, *J* = 7.8 Hz, 1H), 7.43 (d, *J* = 3.2 Hz, 3H). ^{13}C-NMR (100 MHz, $CDCl_3$ + DMSO-d_6) δ_{ppm} 160.89, 143.51, 133.19, 133.13, 129.11, 128.55, 128.52, 128.38, 125.07, 120.66, 108.59. HRMS (ESI-TOF) (m/z): $[M+H]^+$ Calcd. for: $C_{14}H_9Cl_2N_2OS$ 322.9807; Found 322.9803.

N-(1,3-benzothiazol-2-yl)pyridine-3-carboxamide (C_6).

Yellow solid; yield: 87.5%. M.P: 240–244 °C. *Rf* = 0.57 (ethylacetate/n-hexane, V/V = 3:7). FT-IR (cm^{-1}): 3277 (NH), 3012 (Ar C–H), 1649 (> C=O), 1626 (> C=N), 1589, 1561 (Ar –C=C–), 1511 (amide II), 665 (C–S–C). ^{1}H-NMR (300 MHz, $CDCl_3$ + DMSO-d_6) δ_{ppm} ^{1}H-NMR (400 MHz, DMSO-d_6) δ_{ppm} 13.22 (s, 1H, NH), 8.83 (d, *J* = 5.3 Hz, 2H), 8.03 (t, *J* = 6.8 Hz, 3H), 7.80 (d, *J* = 8.0 Hz, 1H), 7.49 (t, *J* = 7.6 Hz, 1H), 7.36 (t, *J* = 7.5 Hz, 1H). ^{13}C-NMR (100 MHz, $CDCl_3$ + DMSO-d_6) δ_{ppm} 170.02, 164.17, 157.72, 154.61, 152.73, 140.85, 136.56, 133.18, 130.91, 128.61, 128.23, 126.18, 125.16. HRMS (ESI-TOF) (m/z): $[M+H]^+$ Calcd. for: $C_{13}H_{10}N_3OS$ 256.0545; Found: 256.0536.

N-(1,3-benzothiazol-2-yl)pyridine-4-carboxamide (C_7).

Yellow solid; yield: 86.4%. M.P: 242–244 °C. *Rf* = 0.67 (ethylacetate/n-hexane, V/V = 3:7). FT-IR (cm^{-1}): 3279 (NH), 3018 (Ar C–H), 1654 (> C=O), 1632 (> C=N), 1595, 1562 (Ar –C=C–), 1519 (amide II), 665 (C–S–C). ^{1}H-NMR (400 MHz, DMSO-d_6) δ_{ppm} 13.23 (s, 1H, NH), 8.84 (d, *J* = 5.3 Hz, 2H), 8.04 (t, *J* = 6.8 Hz, 3H), 7.81 (d, *J* = 8.0 Hz, 1H), 7.50 (t, *J* = 7.6 Hz, 1H), 7.37 (t, *J* = 7.5 Hz, 1H). ^{13}C-NMR (100 MHz, DMSO-d_6) δ_{ppm} ^{13}C-NMR (100 MHz, DMSO-d_6) δ_{ppm} 165.69, 159.59, 150.95, 148.11, 139.83, 131.72, 126.86, 124.44, 122.37, 120.64. HRMS (ESI-TOF) (m/z): $[M+H]^+$ Calcd. for: $C_{13}H_{10}N_3OS$ 256.0539; Found 256.0536.

N-(1,3-benzothiazol-2-yl)-1H-indole-2-carboxamide (C_8).

White powder; yield: 82.5%. M.P: 276–278 °C. *Rf* = 0.68 (ethylacetate/n-hexane, V/V = 2:8). FT-IR (cm^{-1}): 3327 (NH), 3028 (Ar C–H), 1651 (> C=O), 1633 (> C=N), 1590, 1559 (Ar –C=C–), 1528 (amide II), 669 (C–S–C). ^{1}H-NMR (400 MHz, DMSO-d_6) δ_{ppm} 12.94 (s, 1H, NH), 11.98 (s, 1H, NH), 8.03 (d, *J* = 7.6 Hz, 1H), 7.80 (d, *J* = 8.1 Hz, 1H), 7.76–7.67 (m, 2H), 7.52–7.43 (m, 2H), 7.38–7.31 (m, 1H), 7.28 (ddd, *J* = 8.2, 7.0, 1.0 Hz, 1H), 7.10 (t, *J* = 7.1 Hz, 1H). ^{13}C-NMR (100 MHz, $CDCl_3$ + DMSO-d_6) δ_{ppm} 164.79, 163.59, 153.58, 142.45, 136.95, 134.10, 132.13, 130.69, 129.72, 128.27, 127.18, 125.96, 125.18, 117.28, 112.29, 15.08. HRMS (ESI-TOF) (m/z): $[M+H]^+$Calcd. for: $C_{16}H_{12}N_3OS$ 294.0695; Found: 294.0690.

N-(1,3-benzothiazol-2-yl)-2-iodobenzamide (C_9).

White powder; yield: 86.9.5%. M.P: 180–182 °C. *Rf* = 0.69 (ethylacetate/n-hexane, V/V = 3:7). FT-IR (cm^{-1}): 3289 (NH), 3017 (Ar C–H), 1655 (> C=O), 1618 (> CN), 1596, 1559 (Ar –C=C–), 1509 (amide II), 670 (C–S–C). ^{1}H-NMR (400 MHz, DMSO-d_6) δ_{ppm} 12.87 (s, 1H, NH), 8.04 (d, *J* = 7.7 Hz, 1H), 7.98 (d, *J* = 7.9 Hz, 1H), 7.79 (d, *J* = 8.0 Hz, 1H), 7.59 (dd, *J* = 7.6, 1.6 Hz, 1H), 7.54 (td, *J* = 7.5, 0.9 Hz, 1H), 7.50–7.44 (m, 1H), 7.39–7.32 (m, 1H), 7.29 (td, *J* = 7.7, 1.7 Hz, 1H). ^{13}C-NMR (100 MHz, DMSO-d_6) δ_{ppm} 168.64, 158.29, 149.02, 140.83, 139.71, 132.41, 132.04, 129.16, 128.61, 126.74, 124.33, 122.29, 121.23, 94.17. HRMS (ESI-TOF) (m/z): $[M+H]^+$ Calcd. for: $C_{14}H_{10}N_2OSI$ 380.9559; Found: 380.9543.

N-(1,3-benzothiazol-2-yl)-2,4-dichlorobenzamide (C_{10}).

White powder; yield: 88.2%. M.P: 208–210 °C. *Rf* = 0.58 (ethylacetate/n-hexane, V/V = 3:7). FT-IR (cm^{-1}): 3288 (NH), 3009 (Ar C–H), 1659 (> C=O), 1622 (> C=N), 1597, 1551 (Ar –C=C–), 1524 (amide II), 668 (C–S–C). ^{1}H-NMR (300 MHz, DMSO-d_6) δ_{ppm} 13.03 (s, 1H, NH), 8.05 (d, *J* = 7.7 Hz, 1H), 7.85–7.77 (m, 2H), 7.75 (s, 1H), 7.60 (dd, *J* = 8.3, 1.9 Hz, 1H), 7.52–7.44 (m, 1H), 7.36 (t, *J* = 7.6 Hz, 1H). ^{13}C-NMR (100 MHz, DMSO-d_6) δ_{ppm} 165.40, 158.24, 148.76, 136.46, 133.54, 132.15, 131.94, 131.46, 129.96, 128.02, 126.81, 24.43, 122.35, 121.18. HRMS (ESI-TOF) (m/z): $[M+H]^+$ Calcd. for: $C_{14}H_9Cl_2N_2OS$ 322.9807; Found: 322.9803.

N-(1,3-benzothiazol-2-yl)-2-phenoxyacetamide (C_{11}).

White powder; yield: 83.8%. M.P: 156–158 °C. *Rf* = 0.67 (ethylacetate/n-hexane, V/V = 4:6). FT-IR (cm^{-1}): 3276 (NH), 3010 (Ar C–H), 2834 (CH_2), 1650 (> C=O), 1626 (> C=N), 1589, 1564 (Ar –C=C–), 1515 (amide II), 1031, 1228 (C–O–C), 672 (C–S–C). ^{1}H-NMR (400 MHz, DMSO-d_6) δ_{ppm} 12.60 (s, 1H, NH), 8.00 (d, *J* = 7.6 Hz, 1H), 7.78 (d, *J* = 8.0 Hz, 1H), 7.49–7.43 (m, 1H), 7.36–7.29 (m, 3H), 6.99 (dd, *J* = 8.4, 7.7 Hz, 3H), 4.93 (s, 2H). ^{13}C-NMR (100 MHz, DMSO-d_6) δ_{ppm} 168.38, 158.17, 157.87, 148.93, 131.94, 130.05, 126.70, 124.22, 122.27, 121.77, 121.13, 115.03, 66.58. HRMS (ESI-TOF) (m/z): $[M+H]^+$ Calcd. for: $C_{15}H_{13}N_2O_3S$ 285.0703; Found: 285.0709.

N-(1,3-benzothiazol-2-yl)-2-methoxybenzamide (C_{12}).

White powder; yield: 90.5%. M.P: 156–158 °C. *Rf* = 0.71 (ethylacetate/n-hexane, V/V = 3:7). FT-IR (cm^{-1}): 3283 (NH), 2928 (CH_2), 3011 (Ar C–H), 1655 (> C=O), 1621 (> C=N), 1590, 1558 (Ar–C=C–), 1519 (amide II), 1032, 1255 (C–O–C), 667 (C–S–C). ^{1}H-NMR (400 MHz, DMSO-d_6) δ_{ppm} 12.05 (s, 1H, NH), 8.02 (d, *J* = 7.9 Hz, 1H), 7.81–7.74 (m, 2H), 7.60 (t, *J* = 7.8 Hz, 1H), 7.47 (t, *J* = 7.6 Hz, 1H), 7.34 (t, *J* = 7.6 Hz, 1H), 7.25 (d, *J* = 8.4 Hz, 1H), 7.12 (t, *J* = 7.5 Hz, 1H), 3.96 (s, 3H, OCH_3). ^{13}C-NMR (100 MHz, DMSO-d_6) δ_{ppm} 165.27, 158.14, 157.73, 149.04, 134.21, 132.12, 130.88, 126.69, 124.17, 122.24, 121.91, 121.21, 121.07, 112.80, 56.65. HRMS (ESI-TOF) (m/z): $[M+H]^+$ Calcd. for: $C_{15}H_{13}N_2O_3S$ 285.0692; Found: 285.0687.

N-(1,3-benzothiazol-2-yl)thiophene-2-carboxamide (C_{13}).

White powder; yield: 84.7%. M.P: 208–210°. *Rf* = 0.76 (ethylacetate/n-hexane, V/V = 4:6). FT-IR (cm^{-1}): 3284 (NH), 3016 (Ar C–H), 1667 (> C=O), 1632 (> C=N), 1598, 1558 (Ar –C=C–), 1532 (amide II), 671 (C–S–C). ^{1}H-NMR (300 MHz, DMSO-d_6) δ_{ppm} 13.03 (s, 1H, NH), 8.32 (s, 1H), 8.02 (d, *J* = 6.5 Hz, 2H), 7.78 (d, *J* = 7.3 Hz, 1H), 7.48 (t, *J* = 7.6 Hz, 1H), 7.36 (d, *J* = 7.7 Hz, 1H), 7.30 (dd, *J* = 8.3, 4.1 Hz, 1H). ^{13}C-NMR (100 MHz, DMSO-d_6) δ_{ppm} 159.70, 157.94, 148.02, 136.93, 136.32, 133.58, 130.86, 128.11, 125.68, 123.12, 121.22, 119.74. HRMS (ESI-TOF) (m/z): $[M+H]^+$ Calcd. for: $C_{12}H_9N_2O_2S$ 261.0156; Found: 261.0145.

N-(1,3-benzothiazol-2-yl)quinoline-2-carboxamide (C_{14}).

White powder; yield: 88.8%. M.P: 176–178 °C. *Rf* = 0.59 (ethylacetate/n-hexane, V/V = 4:6). FT-IR (cm^{-1}): 3269 (NH), 3018 (Ar C-H), 1654 (> C=O), 1633, 1621 (> C=N), 1598, 1557 (Ar –C=C–), 1514 (amide II), 669 (C-S-C). ^{1}H-NMR (300 MHz, DMSO-d_6) δ_{ppm} 12.50 (s, 1H, NH), 8.70 (d, *J* = 8.5 Hz, 1H), 8.30 (dd, *J* = 8.4, 4.7 Hz, 2H), 8.16 (d, *J* = 8.2 Hz, 1H), 8.09 (d, *J* = 7.8 Hz, 1H), 7.96 (t, *J* = 7.7 Hz, 1H), 7.83 (dd, *J* = 16.8, 8.2 Hz, 2H), 7.51 (t, *J* = 7.6 Hz, 1H), 7.39 (t, *J* = 7.5 Hz, 1H). ^{13}C-NMR (100 MHz, DMSO-d_6) δ_{ppm} 164.09, 157.96, 149.09, 148.20, 146.52, 138.96, 132.22, 131.43, 130.10, 129.81, 129.46, 128.63, 126.83, 124.46, 122.41, 121.28, 119.38. HRMS (ESI-TOF) (m/z): $[M+H]^+$ Calcd. for: $C_{17}H_{12}N_3OS$ 306.0701; Found 306.0691.

N-(1,3-benzothiazol-2-yl)-2-(1H-indol-2-yl)acetamide (C_{15}).

White powder; yield: 86.5%. M.P: 180–184 °C. *Rf* = 0.78 (ethylacetate/n-hexane, V/V = 6:4). FT-IR (cm^{-1}): 3311 (NH), 3020 (Ar C–H), 1663 (> C=O), 1619 (> C=N), 1594, 1563 (Ar –C=C–), 1529 (amide II), 668 (C–S–C). ^{1}H-NMR (400 MHz, DMSO-d_6) δ_{ppm} 12.55 (s, 1H, NH), 10.99 (s, 1H, NH), 7.95 (d, *J* = 7.6 Hz, 1H), 7.74 (d, *J* = 8.0 Hz, 1H), 7.62 (d, *J* = 7.8 Hz, 1H), 7.43 (t, *J* = 7.7 Hz, 1H), 7.38 (d, *J* = 8.1 Hz, 1H), 7.34–7.26 (m, 2H), 7.09 (t, *J* = 7.5 Hz, 1H), 7.01 (t, *J* = 7.4 Hz, 1H), 3.94 (s, 2H). ^{13}C-NMR (100 MHz, DMSO-d_6) δ_{ppm} 171.19 (> C=O), 158.58, 149.03, 136.58, 131.93, 127.60, 126.55, 124.84, 123.95, 122.15, 121.62, 120.95, 119.07, 111.95, 107.70, 67.77, 32.93 (CH_2). HRMS (ESI-TOF) (m/z): $[M+H]^+$ Calcd.for:$C_{17}H_{12}N_3OS$ 308.0858; Found: 308.0847.

N-(1,3-benzothiazol-2-yl)-4-oxo-3,4-dihydro-2H-chromene-3-carboxamide (C_{16}).

Yellow powder; yield: 85.2%. M.P: 250–252 °C. *Rf* = 0.70 (ethylacetate/n-hexane, V/V = 6:4). FT-IR (cm^{-1}): 3297 (NH), 3018 (Ar C–H), 1721 (> C=O), 1647 (> C=O), 1630 (> C=N), 1594, 1567 (Ar –C=C–), 1521 (amide II), 1030, 1244 (C–O–C), 661 (C–S–C). ^{1}H-NMR (400 MHz, $CDCl_3$) δ_{ppm} 9.11 (s, 1H, NH), 8.39 (dd, *J* = 8.0, 1.6 Hz, 1H), 7.90–7.80 (m, 3H), 7.64–7.55 (m, 2H), 7.47 (td, *J* = 8.3, 7.3, 1.2 Hz, 1H), 7.33 (td, *J* = 7.8, 1.1 Hz, 1H), 5.30 (s, 3H). ^{13}C-NMR (100 MHz, $CDCl_3$) δ_{ppm} 176.66, 163.35, 156.83, 156.15, 135.30, 132.65, 126.94, 126.64, 126.27, 124.04, 121.51, 121.32, 118.56, 114.33, 71.95, 53.46, 31.84. HRMS (ESI-TOF) (m/z): $[M-H]^+$ Calcd. for: $C_{17}H_{11}N_2O_3S$ 323.3537; Found: 323.0483.

N-(1,3-benzothiazol-2-yl)-3-bromobenzamide (C_{17}).

White powder; yield: 88.6%. M.P: 160–164 °C. *Rf* = 0.64 (ethylacetate/n-hexane, V/V = 3:7). FT-IR (cm^{-1}): 3269 (NH), 3012 (Ar C–H), 1657 (> C=O), 1632 (> C=N), 1596, 1558 (Ar –C=C–), 1535 (amide II), 670 (C–S–C). ^{1}H-NMR (500 MHz, DMSO-d_6) δ_{ppm} 13.09 (s, 1H, NH), 8.36 (s, 1H), 8.15 (d, *J* = 7.9 Hz, 1H), 8.08–8.01 (m, 1H),

7.87 (d, $J = 8.0$ Hz, 1H), 7.80 (d, $J = 8.0$ Hz, 1H), 7.54 (t, $J = 7.9$ Hz, 1H), 7.49 (t, $J = 7.7$ Hz, 1H), 7.36 (t, $J = 7.6$ Hz, 1H). ^{13}C-NMR (100 MHz, DMSO-d_6) δppm 166.45, 135.92, 134.80, 132.23, 131.80, 131.50, 131.28, 128.75, 127.91, 126.75, 124.28, 122.34, 122.30, 120.64. HRMS (ESI-TOF) (m/z): $[M+H]^+$ Calcd. for: $C_{14}H_8N_2OSBr$ 332.9697; Found: 332.9686.N-(1,3-benzothiazol-2-yl)-2-methylbenzamide (C_{18}).

White powder; yield: 92.5%. M.P: 160–162 °C. $Rf = 0.62$ (ethylacetate/n-hexane, V/V = 2:8). FT-IR (cm^{-1}): 3265 (NH), 3021 (Ar C–H), 2969 (CH_3), 1653 (> C=O), 1628 (> C=N), 1591, 1558 (Ar –C=C–), 1517 (amide II), 665 (C–S–C). ^{1}H-NMR (500 MHz, DMSO-d_6) δ_{ppm} 12.76 (s, 1H, NH), 8.02 (d, $J = 7.9$ Hz, 1H), 7.80 (dd, $J = 16.1$, 7.5 Hz, 1H), 7.62 (d, $J = 7.4$ Hz, 1H), 7.48–7.41 (m, 1H), 7.38–7.32 (m, 1H), 7.31–7.26 (m, 1H), 2.52 (s, 1H), 2.44 (s, 3H). ^{13}C-NMR (100 MHz, DMSO-d_6) δ_{ppm} 158.68, 148.96, 139.46, 136.91, 134.25, 131.97, 131.36, 130.65, 128.64, 126.65, 126.22, 124.18, 122.21, 121.03, 20.12. HRMS (ESI-TOF) (m/z): $[M+H]^+$ Calcd. for: $C_{15}H_{13}N_2OS$ 269.0749; Found: 269.0736.

Antibacterial activity assay

Minimum inhibitory concentration (MIC) and minimum bactericidal concentration (MBC)

The antibacterial activity of synthesized compounds $C_{1\text{-}18}$ was screened against four Gram-positive bacterial strains: *Staphylococcus aureus* NCIM 5021 (ATCC 25923), *Staphylococcus aureus* NCIM 5022 (ATCC 29213), methicillin-resistant *Staphylococcus aureus* ATCC 43300 (MRSA), *Staphylococcus epidermidis* NCIM 2493; *Klebsiella pneumoniae* NCIM 2706, *Pseudomonas aeruginosa* NCIM 2036, *Escherichia coli* NCIM 2065 and *Mycobacterium Sp.* NCIM 2984, using the guidelines of Clinical Laboratories Standard Institute (CLSI 2007). *S. aureus* NCIM 5021 strain used in this study is sensitive to methicillin, amikacin, ampicillin, bacitracin and benzyl penicillin, while *S. aureus* NCIM 5022 is sensitive to methicillin, ampicillin, carbenicillin, cephalothin, chloroamphenicol, clindamycin, colistin, erythromycin, gentamycin, kanamycin, nitrofurantoin, penicillin G and tetracycline. These two strains are used as the reference strains for susceptibility testing of different antibiotics. The clinical isolate *S. aureus* ATCC 43300 is an oxacillin- and methicillin-resistant strain.

All tests were carried out by the broth microdilution method in Mueller Hinton medium (Hi-media) using 96-well microtitre plates. Compounds $C_{1\text{-}18}$ dissolved in sterile dimethyl sulphoxide (DMSO) were used to screen their antibacterial activity, while standard drugs ciprofloxacin and gentamicin in sterile DMSO were used as a positive control. Sterile DMSO is served as a negative control. One hundred microlitres was the final volume for MIC protocols, and DMSO concentration in each assay well was below 1%. All synthesized compounds dissolved in sterile DMSO were screened against the selected strains in the concentration range of 0.39–125 µg/mL. Corresponding wells were inoculated with the bacterial suspensions at 10^5 colony-forming unit/mL (CFU/mL) concentrations, and then, 96-well microtitre plates were incubated without agitation at 37 °C for 24 h. After incubation period plates were agitated, the absorbance was measured at 600 nm. Tests were carried out in triplicate, and results were taken as a mean. For the MBC determination, an aliquot of 50 µl from each well was pipetted out and sub-cultured on sterile Mueller–Hinton agar plates. These plates were further incubated for 24 h at 37 °C, and the numbers of colony were counted using colony counter (Manti Lab, M316, India). The lowest concentrations of the test compound that did not produce any bacterial growth on agar plates were regarded as the MBC values (Pankey and Sabath, 2004). For each strain, all experiments were performed in triplicate. The ratio MBC/MIC ≤ 2 is usually regarded as the bactericidal activity, while the MBC/MIC ratio ≥ 4 is considered as bacteriostatic activity of test compound (Levison 2004). The results of MIC and MBC determinations of the tested compounds are presented in Table 3 and Table 4, respectively.

Time-kill assay

Compounds C_9 and C_{14} exhibited low MIC values against *S. aureus* NCIM 5021, while compound C_{13} displayed most potent activity against *S. aureus* ATCC 43300. These three compounds were selected for their time-kill kinetic assays. Time-kill assays were performed by the broth macro-dilution method according to the guidelines of Clinical Laboratories Standard Institute (CLSI 2007). *S. aureus* NCIM 5021 and *S. aureus* ATCC 43300 inoculum suspensions were serially diluted to the concentration of 10^5 CFU/mL. The inoculum suspensions of *S. aureus* NCIM 5021 were treated with test compounds **C_9** (at test concentrations of 9.8 and 19.7 µM) and **C_{14}** (at test concentrations of 12.7 and 25.5 µM), whereas inoculum suspensions of *S. aureus* ATCC 43300 were treated with compound C_{13} at test concentrations of 7.5 and 15 µM. Ciprofloxacin was kept as a positive control at test concentrations of 47.9 and 95.9 µM. The treated inoculum cultures were then incubated at 37 °C, and at timed intervals (0, 2, 4, 6, 8, 12, and 24 h) 50 µL from the corresponding cultures was collected and subsequently sub-cultured on nutrient agar medium. Plates were incubated at 37 °C for 24 h, and then, CFUs were determined (Supplementary Table S1). All data were analysed by constructing $\log_{10}$ CFU per millilitre versus time (h) plot (Fig. 2a–c).

Compared to the initial inoculums, a reduction of ≥ 3 $\log_{10}$ CFU/mL indicates the bactericidal activity, while < 3 $\log_{10}$ CFU/mL corresponds to the bacteriostatic activity.

Cytotoxicity and selective index

The cytotoxic activity of compounds $C_{1\text{-}18}$ was evaluated according to the 3-(4,5-dimethyl-2-thiazolyl)-

2,5-diphenyl-2H-tetrazolium bromide (MTT) assay protocol published by the American Type Culture Collection (ATCC) on VERO Cells (ATCC CCL-81) using dimethyl sulphoxide (DMSO) as a negative control under the same dilution conditions. Experiments were repeated three times. Activities were expressed as the concentration of drug inhibiting 50% cell growth (IC_{50}) and are summarized in Table 5.

Results and discussion

In the present study, we synthesized eighteen new N'-(1,3-benzothiazol-2-yl)-substituted arylamides as outlined in Scheme 1. HOBt- and EDCl-catalysed reaction of 1,3-benzothiazole-2-amine (A) with appropriate substituted aromatic acids in dimethyl formamide (DMF) (Larsen et al. 2011) afforded title compounds 1–18 in 80.2–94.2% yield. Optimization of the reaction conditions for the synthesis of titled compounds 1–18 started by reacting 1,3-benzothiazole-2-amine (A) with 2-fluorobenzoic acid as model substrate with different amounts of catalyst and solvents at varied temperatures (Table 1). The reaction was carried out under stirring in the presence of 2.0 equivalent each of HOBt and EDCl using acetonitrile as a solvent. The desired product C_1 (Scheme 1) was achieved only in 25.3% yield (Table 1, entry 1). This inspired us to further examine the optimal reaction conditions for a more satisfactory result. We also investigated the effect of solvent on the yield of the product. Changing the solvent from CH_3COCH_3 to tetrahydrofuran (THF) did not improve the reaction yield (Table 1, entry 2–5). The highest yield was obtained when DMF was used as solvent at room temperature (Table 1, entry 6). The amount of catalyst was also investigated, and an amount of 2.0 equivalent each of HBOt and EDCl was observed to the best one, affording the product in 85.6% yield. Decreasing the mount of catalyst, 1.5 equivalent each of HBOt and EDCl did not improve the reaction yield (Table 1, entry 7).

The structures of newly synthesized compounds $\mathbf{C_{1\text{-}18}}$ (Table 2) have been characterized by ^{1}H-NMR, ^{13}C-NMR and HRMS spectral data (Supplementary Figs. S1-18). In the Fourier transform infrared (FT-IR) spectra of compounds $C_{1\text{-}18}$, characteristic absorption bands of amide NH and > C=O appeared, respectively, in the region 3224–3327 cm^{-1} and 1648–1667 cm^{-1}, whereas the

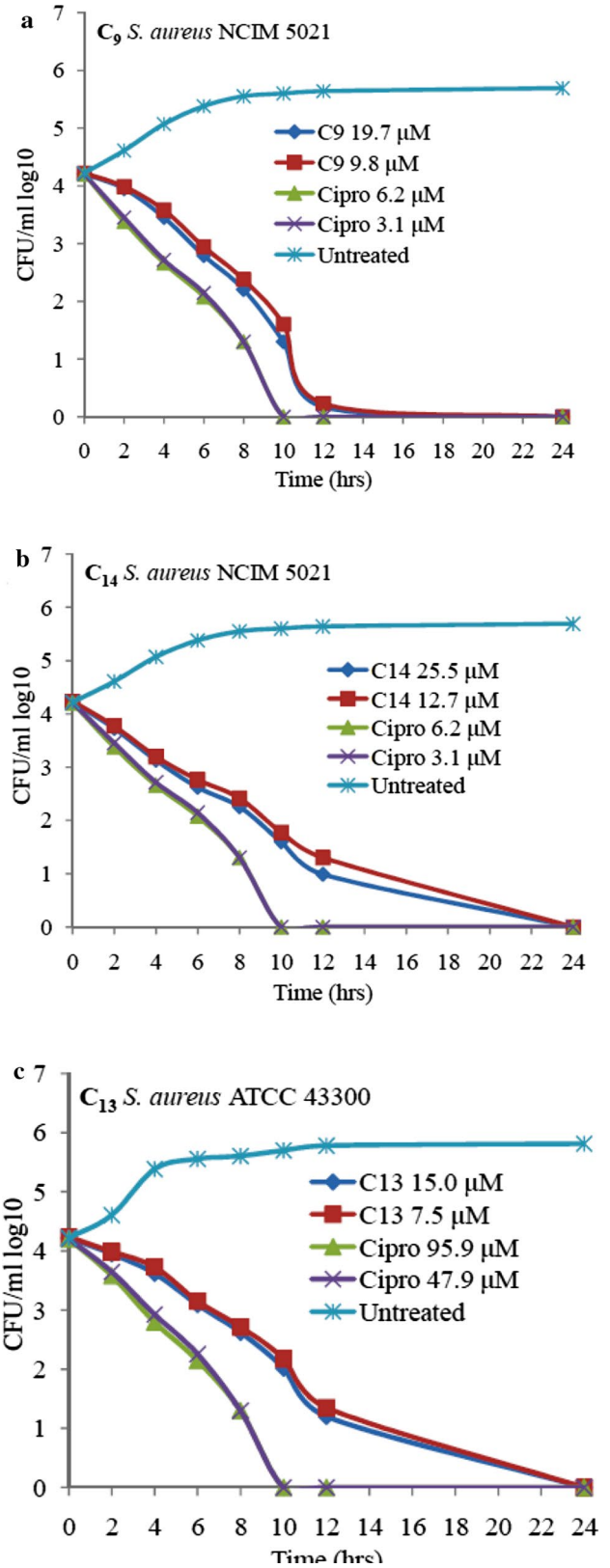

Fig. 2 Plots represent the time-kill profile of compounds **a** 9 **b** 14 and **c** 13

stretching absorption bands of benzothiazole ring > C=N and C–S–C functions were observed, respectively, in the regions of 1612–1633 cm^{-1} and 661–675 cm^{-1}. Further, the formation of compounds $C_{1\text{-}18}$ was supported by the disappearance of carboxylic > C=O and OH peaks and the appearance of amide > C=O peaks in the range between 1648 and 1667 cm^{-1}.

Formation of compounds $C_{1\text{-}18}$ was supported by their ^{1}H-NMR spectra, which showed amide NH signals in the region δ 8.84–13.22 ppm. However, in compounds C_2, C_3 and C_5 signals due to NH protons did not appear, which may be due to the replacement of exchangeable protons with deuterium. In the ^{1}H-NMR spectra, splitting patterns for the aromatic protons were observed to be in agreement with the substitution pattern of respective compounds. The chemical shift values and coupling constant (*J* values) of aromatic protons were assigned accordingly with the position of aromatic protons. Aromatic protons on coupling with ortho and meta protons exhibited characteristic splitting patterns such as double doublet (dd), triplet of doublet (td), triplet (t) and doublet (d). In the ^{1}H-NMR spectrum of representative compound C_1, eight aromatic protons appeared in the region at δ 7.28–7.99 ppm (Supplementary Fig. S1a and S1b). A sharp singlet signal that appeared at δ 12.86 ppm is ascribed to the NH proton. In this compound, proton present on position four of benzothiazole ring appeared as doublet at δ 7.99 ppm ($J = 7.3$, 1.7 Hz), while a multiplet signal appeared at δ 7.25–7.38 ppm is due to three protons present on position five, six and seven of this ring. ^{1}H spectrum of compound C_1 showed H···F interactions for H3′, H4′, H5′ and H6′ and observed to be typical through bond coupling. A double doublet that appeared at δ 7.76 ppm is assigned to H3′ and H4′ coupled to ^{19}F with *J* value of 91.45 Hz. A triple of doublet that appeared at δ 7.61 ppm is assigned to H6′ couplet to ^{19}F with *J* value of 73.17 Hz. The multiplet that appeared at δ 7.39–7.46 ppm is due to H5′ of fluorobenzene ring. In the ^{13}C NMR spectrum of compound C_1, the carbonyl carbon of amide function exhibited a singlet signal at δ 161.69 ppm, while the azomethine carbon of the benzothiazole ring appeared as a singlet at δ 160.69 ppm (Supplementary Fig. S1c-d). For compound C_1 ^{13}C-^{19}F coupling was observed as doublet, one bond distance $^{1}JCF = 134.86$ Hz and at two bonds distance $^{2}JCF = 118.63$ and 116.19 Hz. These were assigned to coupling of ^{13}F with to C-2′ at δ 134.86 ppm, with coupling to C1′ at δ 118.63 ppm, and with coupling to C3′ at δ 116.19 ppm, respectively (Supplementary Fig.S1e). Remaining nine SP^2-hybridized aromatic carbons appeared at their expected region between δ 116.07–159.21 ppm. In the ^{19}F NMR spectrum (Supplementary Fig. S1d), fluorine atom appeared as singlet signal at δ -113.27 ppm. In the mass spectrum of compound C_1 $[M + H]^+$ peak was observed at m/z 273.0489 (100%), which corresponds to its molecular formula $C_{14}H_9N_2OSF$ (Supplementary Fig. S1e). In the ^{13}C-NMR spectrum of all other compounds, the carbonyl carbon of benzamide and azomethine carbon of benzothiazole ring appeared in the range, respectively, at δ 162.09–176.66 and δ 134.38–161.33 ppm. Also, aromatic SP^2-hybridized carbon signals in all other compounds appeared in the expected region.

Minimum inhibitory concentration (MIC)

Antibacterial activity of synthesized compounds $C_{1\text{-}18}$ was evaluated by the broth microdilution method (CLSI 2007) using Mueller Hinton medium (HiMedia). The MIC value of tested compounds is presented in Table 3 and compared with the standard drugs ciprofloxacin. Compounds $C_{1\text{-}18}$ exhibited variable activity against the tested Gram-positive and Gram-negative bacterial strains. Among all tested compounds, C_3, C_5, C_9, $C_{13\text{-}15}$ and C_{17} exhibited significant activity against *S. aureus* NCIM 5021 with MIC values in the range of 19.7–30.3 µM, while other tested compounds showed moderate-to-low activity (MIC, 48.4 to 114 µM) against this strain. Against *S. aureus* NCIM 5022 only four compounds, i.e. C_1, C_3, C_{13}, C_{16} and C_{17}, showed promising activity (MIC, 13 to 30 µM) against *S. aureus* NCIM 5022 compared to the standard drugs ciprofloxacin (MIC 6.3 µM) and gentamycin (MIC, 16.9 µM). Among all tested compounds C_{13} possessing thiophene ring attached to the benzothiazole moiety via amide linkage exhibited maximum activity against this strain with MIC of 13 µM. It is evident from result that two electron-withdrawing groups at positions two and six of the phenyl ring (compound **C_5** MIC, 197.3 µM) decrease activity against *S. aureus* NCIM 5022. In compound C_6, 3-pyridyl ring attached to the amide function also decreased activity (MIC, 249 µM) against this strain. This may be due to the presence of the electronegative nitrogen in the pyridine ring making this ring system relatively electron-deficient in compound C_6. Also, large aromatic ring systems like indole (compound C_8 MIC, 106 µM) and quinoline (compound C_{14} MIC, 102.2 µM) and also alkaryl group (compound C_{11} MIC, 110 µM) when attached to the benzothiazole ring via amide linkage decreased the activity against *S. aureus* NCIM 5022. Against *S. aureus* ATCC 43300 (MRSA), compounds C_1, C_3, C_5, C_6, C_9, C_{10} and $C_{13\text{-}16}$ showed potent activity (MIC, 15.0–26.4 µM), while all other tested compounds exhibited moderate-to-low activity (MIC, 44.2–114 µM). Compound C_{13} possessing thiophene ring showed maximum activity against *S. aureus* ATCC 43300 (MIC, 15.0 µM). It is evident that the substitution of electronegative halogen atom either on ortho or para position of the phenyl ring (C_1, C_3, C_5, C_9 and C_{10}) attached to the benzothiazole moiety via amide linkage is optimum for activity against this strain. It is also observed that larger heterocyclic rings (compounds C_8, C_{14} and C_{16}) are also well tolerated for activity against *S. aureus* ATCC 43300.

Table 3 Antibacterial screening result of synthesized compounds $\mathbf{C_{1\text{-}18}}$ against selected Gram-positive and Gram-negative bacteria

Comp	Minimum inhibitory concentration (μM)*							
	[a]*S.a*	[b]*S. a*	[c]*S.a*	[d]*S.e*	[e]*M. t*	[f]*K. p*	[g]*P. a*	[h]*E. c*
C_1	110 ± 1.12	30.1 ± 0.97	26.4 ± 0.49	58.0 ± 0.25	29.7 ± 0.45	26.4 ± 0.49	57.3 ± 0.12	57.3 ± 0.15
C_2	114 ± 1.2	56.7 ± 0.49	114 ± 1.2	57.0 ± 0.49	113 ± 1.12	56.7 ± 0.49	54.1 ± 0.97	113 ± 0.97
C_3	21.5 ± 0.49	23.3 ± 0.49	23.3 ± 0.25	91.1 ± 0.54	95.8 ± 1.12	45.5 ± 0.25	94.3 ± 0.54	45.8 ± 0.15
C_4	106 ± 0.49	102 ± 1.2	102.1 ± 1.2	102.3 ± 0.54	106 ± 0.45	106 ± 0.54	206 ± 0.54	108 ± 0.97
C_5	24.2 ± 0.49	197 .3 ± 1.2	22.3 ± 0.54	48.4 ± 0.12	96.5 ± 0.45	49.2 ± 0.25	96.3 ± 0.54	23.9 ± 0.15
C_6	57.4 ± 1.2	249 ± 1.2	29.3 ± 0.49	60.2 ± 0.49	128 ± 1.2	29.5 ± 0.25	238 ± 0.97	122 ± 0.25
C_7	58.2 ± 0.97	129 ± 1.2	57.2 ± 1.2	121.1 ± 0.97	32.3 ± 1.2	126.3 ± 0.54	123 ± 0.54	120 ± 0.97
C_8	52.6 ± 0.49	106 ± 0.25	53.3 ± 0.25	55.4 ± 0.94	104 ± 0.54	25.4 ± 0.49	209 ± 0.54	212 ± 1.2
C_9	19.7 ± 0.97	161.3 ± 1.2	21.0 ± 1.2	82.8 ± 0.25	163.1 ± 0.54	40.2 ± 0.54	165 ± 0.25	164 ± 0.97
C_{10}	99.3 ± 1.12	95.6 ± 0.49	23.9 ± 0.25	22.6 ± 1.12	97.2 ± 0.12	46.8 ± 1.2	194 ± 0.12	24.2 ± 0.15
C_{11}	110 ± 1.12	110 ± 0.12	28.1 ± 1.2	109 ± 0.25	111 ± 0.12	52.81 ± 0.54	115 ± 0.97	112 ± 0.54
C_{12}	54.2 ± 0.49	112 ± 0.25	28.5 ± 1.12	112.3 ± 0.54	217 ± 0.97	55.6 ± 0.49	221 ± 0.49	112 ± 0.54
C_{13}	30.3 ± 0.49	13.0 ± 0.49	15.0 ± 0.25	29.6 ± 0.12	57.6 ± 0.54	27.1 ± 0.97	118 ± 0.54	30.7 ± 0.25
C_{14}	25.5 ± 0.97	102.2 ± 0.12	26.2 ± 0.25	99.3 ± 1.12	206 ± 0.49	102 ± 0.25	202 ± 0.49	205 ± 0.25
C_{15}	24.4 ± 0.49	51.7 ± 0.49	23.7 ± 0.49	12.7 ± 0.12	201 ± 0.49	51.7 ± 0.25	104 ± 0.54	99.6 ± 1.12
C_{16}	48.4 ± 0.49	25.0 ± 0.54	21.9 ± 0.54	23.4 ± 0.25	191 ± 0.54	22.2 ± 0.54	192 ± 0.45	47.8 ± 0.25
C_{17}	23.1 ± 0.49	22.2 ± 1.2	44.2 ± 0.54	23.1 ± 0.25	189 ± 0.49	21.9 ± 0.54	98.4 ± 0.54	95.4 ± 0.25
C_{18}	59.3 ± 0.49	58.2 ± 0.25	119 ± 0.97	53.7 ± 1.2	112 ± 1.2	57.0 ± 0.54	229 ± 0.54	114 ± 1.2
Cipro floxacin	6.2 ± 0.82	6.3 ± 0.52	95.9 ± 0.78	6.3 ± 0.52	3.6 ± 0.52	6.6 ± 0.76	1.6 ± 0.94	6.9 ± 0.52
Genta micin	17.1 ± 0.99	16.9 ± 0.92	41.2 ± 0.78	17.1 ± 0.98	16.9 ± 0.62	2.3 ± 0.88	4.6 ± 0.83	2.0 ± 0.52

*Values are mean ± SEM ($n = 3$)

Ciprofloxacin and Gentamicin used as positive control

[a]*S. a: Staphylococcus aureus* NCIM 5021; [b]*S. a: Staphylococcus aureus* NCIM 5022;[c]*S. a: Methicillin resistant Staphylococcus aureus* ATCC 43,300 (MRSA); [d]*S. e: Staphylococcus epidermidis NCIM* 2493; [e]*M.t. a:Mycobacterium sp.* NCIM 2984; [f]*K. p: Klebsiella pneumoniae* NCIM 2706; [g]*P. a: Pseudomonas aeruginosa* NCIM 2036; [h]*E. c: Escherichia coli* NCIM 2065

MIC: Minimum inhibitory concentration

On the other hand, five compounds, i.e. C_{10}, C_{13} and $C_{15\text{-}17}$, showed significant activity (MIC, 12.7–29.6 μM) against *S. epidermidis* NCIM 2493, while all other tested compounds exhibited moderate-to-low activity (MIC, 48.4–121.1 μM). Maximum activity against this strain was observed with compound C_{15} (MIC, 12.7 μM) possessing indole nucleus attached to the benzothiazole moiety via actamide linkage. Except C_1 and C_7, which showed promising activity (MIC, 29.7 and 32.3 μM), all other tested compounds showed moderate-to-low activity (MIC, 57.6–217 μM) against *Mycobacterium sp.* NCIM 2984. Six tested compounds C_1, C_6, C_8, C_{13}, C_{16} and C_{17} showed promising activity against *K. pneumoniae* NCIM 2706 (MICs, 21.9–29.5 μM), while all other tested compounds displayed moderate-to-low activity (MIC, 45.5–126.3 μM). Moreover, no correlation was observed between substitution pattern and antibacterial activity. In addition, all tested compounds were found to be less active against this strain when compared to the standard drugs ciprofloxacin (MIC 6.6 μM) and gentamycin (MIC, 2.3 μM). All tested compounds displayed less activity against *P. aeruginosa* NCIM 2036 (MICs, 54.1–238 μM) compared to the standard drug ciprofloxacin (MIC 1.6 μM) and gentamycin (MIC, 4.6 μM). On the other hand, only three compounds, i.e. C_5, C_{10} and C_{13}, displayed promising activity against *E. coli* NCIM 2065 (MIC, 23.9–30.7 μM). But activities of these tested compounds were observed to be far less when compared to the standard drugs ciprofloxacin (MIC, 6.9 μM) and gentamicin (MIC, 2 μM). It is evident from the above results that tested compounds are more active against Gram-positive compared to the Gram-negative bacteria. Low activity against Gram-bacteria may be attributed to the poor penetration of test compounds through bacterial cell wall.

Minimum bactericidal concentration (MBC)

MBC values were determined by the broth microdilution method (CLSI 2007) to assess the bactericidal or

Table 4 Minimum bactericidal concentration (MBC) and MBC/MIC ratio of title molecules $\mathbf{C_{1\text{-}18}}$ against selected bacterial strains

Comp	MBC[$*] & MBC/MIC	[a]*S. a*	[b]*S.a*	[c]*MRSA*	[d]*S.e*	[e]*M. t*	[f]*K. P*	[g]*P.a*	[h] *E. c*
$\mathbf{C_1}$	MBC	459.5 ± 0.25	120.5 ± 0.54	105.8 ± 0.54	232.3 ± 0.54	119.1 ± 0.25	108.8 ± 0.29	458.8 ± 0.97	229.4 ± 0.54
	MBC/MIC	4	4	4	4	4	4	8	4
$\mathbf{C_2}$	MBC	223.8 ± 0.54	226.8 ± 0.89	229.8 ± 1.21	228.2 ± 0.1.30	405.3 ± 0.97	203.3 ± 0.89	193.9 ± 0.56	415.3 ± 0.97
	MBC/MIC	2	4	2	4	4	4	4	4
$\mathbf{C_3}$	MBC	86.3 ± 0.88	93.4 ± 0.25	186.9 ± 0.74	182.2 ± 0.54	383.4 ± 0.97	182.2 ± 0.84	188.7 ± 0.90	92.6 ± 0.25
	MBC/MIC	4	4	8	2	4	4	2	2
$\mathbf{C_4}$	MBC	212.7 ± 0.87	416 ± 0.97	416 ± 0.83	204.6 ± 0.99	212.7 ± 0.54	414.7 ± 0.97	414 ± 1.13	436.4 ± 0.54
	MBC/MIC	2	4	4	2	2	4	2	4
$\mathbf{C_5}$	MBC	96.8 ± 1.23	395 ± 0.97	90.6 ± 0.88	192.5 ± 0.92	193.1 ± 0.69	389.4 ± 0.97	386.3 ± 0.94	100.9 ± 0.85
	MBC/MIC	4	2	4	4	2	8	4	4
$\mathbf{C_6}$	MBC	230.5 ± 0.91	498 ± 0.95	119.2 ± 0.79	120.0 ± 0.67	256.4 ± 0.83	119.2 ± 0.90	121.4 ± 0.86	476 ± 0.82
	MBC/MIC	4	2	4	2	2	4	2	4
$\mathbf{C_7}$	MBC	235 ± 0.84	258 ± 0.97	58.8 ± 1.02	230.5 ± 0.78	253.3 ± 0.69	123.56 ± 0.95	495.6 ± 0.77	489 ± 0.97
	MBC/MIC	4	2	4	2	2	4	4	4
$\mathbf{C_8}$	MBC	208.8 ± 0.74	213.6 ± 0.92	215.6 ± 1.22	221.1 ± 0.85	209.5 ± 0.69	213.3 ± 1.21	426.6 ± 0.84	419.7 ± 0.97
	MBC/MIC	4	2	4	4	2	8	2	2
$\mathbf{C_9}$	MBC	39.2 ± 0.65	330.5 ± 0.70	40.81 ± 0.95	331 ± 0.80	326.3 ± 0.79	82.8 ± 0.62	330 ± 1.09	326.3 ± 0.97
	MBC/MIC	2	2	2	4	2	2	2	2
$\mathbf{C_{10}}$	MBC	397.5 ± 0.97	382.6 ± 0.97	47.8 ± 0.25	89.4 ± 0.25	388.8 ± 0.97	194 ± 0.54	338.1 ± 0.89	96.8 ± 0.78
	MBC/MIC	4	4	2	4	4	4	2	4
$\mathbf{C_{11}}$	MBC	440.8 ± 0.69	219.7 ± 0.80	121.1 ± 0.91	219.7 ± 0.82	222.5 ± 0.68	220 ± 0.59	231.6 ± 0.69	442.2 ± 0.88
	MBC/MIC	4	2	4	2	2	4	2	4
$\mathbf{C_{12}}$	MBC	216.9 ± 0.54	450.7 ± 0.97	114 ± 0.25	224.6 ± 0.54	435.2 ± 0.97	110.9 ± 0.54	885.9 ± 1.12	442.2 ± 0.79
	MBC/MIC	4	4	4	2	2	4	4	4
$\mathbf{C_{13}}$	MBC	121.5 ± 0.81	52.3 ± 0.95	30 ± 0.73	122.3 ± 1.25	230.7 ± 0.48	240.3 ± 0.79	475.3 ± 0.68	123 ± 0.89
	MBC/MIC	4	4	2	4	4	8	4	4
$\mathbf{C_{14}}$	MBC	49.8 ± 0.69	204.5 ± 0.74	105.2 ± 0.95	198.6 ± 0.73	412.4 ± 0.97	204.9 ± 0.54	811.8 ± 0.90	410.4 ± 0.87
	MBC/MIC	2	2	4	2	2	2	4	2
$\mathbf{C_{15}}$	MBC	97.7 ± 0.95	207.1 ± 0.54	95.1 ± 0.88	101.6 ± 0.79	406.5 ± 0.97	102.6 ± 1.15	416.9 ± 1.21	405.2 ± 0.97
	MBC/MIC	4	4	4	8	2	2	4	4
$\mathbf{C_{16}}$	MBC	193.8 ± 0.54	96.9 ± 0.88	93.8 ± 0.79	93.8 ± 0.86	765.4 ± 0.73	97.2 ± 0.55	385.1 ± 0.97	191.3 ± 0.98
	MBC/MIC	4	4	4	4	4	4	2	4
$\mathbf{C_{17}}$	MBC	95.7 ± 0.94	86.7 ± 0.87	177.1 ± 0.69	94.2 ± 0.91	756.6 ± 0.90	94.8 ± 0.85	375.9 ± 0.84	190.9 ± 0.90
	MBC/MIC	4	4	4	4	4	4	4	2
$\mathbf{C_{18}}$	MBC	237.3 ± 0.81	232.8 ± 0.88	467.5 ± 0.90	214.9 ± 0.79	225.3 ± 0.93	466.4 ± 0.89	466 ± 0.99	458.2 ± 1.21
	MBC/MIC	4	4	4	4	2	8	2	4
Ciproflox-acin	MBC	2.2 ± 0.85	2.2 ± 0.94	2.0 ± 0.81	2.0 ± 0.78	2.3 ± 0.98	2.1 ± 0.67	2.1 ± 0.80	2.2 ± 0.91
	MBC/MIC	1	< 1	< 1	1	< 1	< 1	< 1	< 1

[*]Values are mean ± SEM ($n = 3$)

Ciprofloxacin used as positive control

[a]*S. a Staphylococcus aureus* NCIM 5021; [b]*S. a Staphylococcus aureus* NCIM 5022;[c]*S. a Methicillin-resistant Staphylococcus aureus* ATCC 43300 (MRSA); [d]*S. e Staphylococcus epidermidis NCIM* 2493; [e]M.*t. a Mycobacterium sp* NCIM 2984; [f]*K. p Klebsiella pneumoniae* NCIM 2706; [g]*P. a Pseudomonas aeruginosa* NCIM 2036; [h]*E. c Escherichia coli* NCIM 2065

MIC minimum inhibitory concentration (μM)

bacteriostatic activity of synthesized compounds $C_{1\text{-}18}$. Amongst all tested compounds, four compounds, i.e. C_2, C_4, C_9 and C_{14}, displayed bactericidal activity (MBC/MIC, 2) (Table 4) against *S. aureus* NCIM 5021, while other tested compounds displayed bacteriostatic activity (MBC/MIC, 4). Against *S. aureus* NCIM 5022, seven compounds ($C_{5\text{-}9}$,

Table 5 Cytotoxic activity (IC_{50}) and selectivity index values of synthesized compounds $\mathbf{C_{1\text{-}18}}$ against tested bacterial strains

Comp	Cytotoxicity IC_{50}-Vero cells (μM)*	Selectivity index (SI) (SI = IC_{50}/MIC**)							
		[a]*S.a*	[b]*S. a*	[c]*S.a*	[d]*S.e*	[e]*M. t*	[f]*K. p*	[g]*P. a*	[h]*E. c*
$\mathbf{C_1}$	250.3 ± 0.88	2.27	8.30	9.46	4.31	8.41	9.48	4.36	4.36
$\mathbf{C_2}$	189.4 ± 0.76	1.65	3.33	1.65	3.31	1.67	3.33	3.49	1.67
$\mathbf{C_3}$	349.3 ± 1.34	16.24	14.99	14.99	3.83	3.63	7.67	3.70	7.61
$\mathbf{C_4}$	104.4 ± 0.55	0.98	1.02	1.02	1.02	0.98	0.98	0.50	0.96
$\mathbf{C_5}$	198.2 ± 1.13	8.18	1.00	8.87	4.09	2.05	4.02	2.05	8.28
$\mathbf{C_6}$	124.4 ± 0.79	4.39	1.01	8.61	4.19	1.97	8.55	1.06	2.06
$\mathbf{C_7}$	152.3 ± 0.85	2.61	1.18	2.66	1.25	4.71	1.20	1.23	1.26
$\mathbf{C_8}$	276.8 ± 0.67	5.26	2.61	5.19	4.99	2.66	10.89	1.32	1.30
$\mathbf{C_9}$	234.3 ± 1.21	11.87	1.45	11.14	2.82	1.43	5.82	1.41	1.42
$\mathbf{C_{10}}$	253.7 ± 0.73	2.55	2.65	10.62	11.23	2.61	5.42	1.30	10.49
$\mathbf{C_{11}}$	277.6 ± 0.95	2.52	2.52	9.89	2.55	2.50	5.26	2.41	2.48
$\mathbf{C_{12}}$	176.2 ± 0.98	3.24	1.57	6.17	1.56	0.81	3.16	0.79	1.57
$\mathbf{C_{13}}$	349.8 ± 1.22	30.32	26.90	23.32	11.81	6.07	12.90	2.96	11.39
$\mathbf{C_{14}}$	198.7 ± 0.89	7.79	1.94	7.58	2.00	0.96	1.94	0.98	0.96
$\mathbf{C_{15}}$	351.6 ± 0.67	14.52	6.80	14.83	27.68	1.74	6.80	3.38	3.53
$\mathbf{C_{16}}$	324.8 ± 0.78	6.71	12.99	14.83	13.80	1.70	14.6	1.69	6.79
$\mathbf{C_{17}}$	152.4 ± 1.06	6.59	6.86	3.44	6.59	0.80	6.95	1.54	1.59
$\mathbf{C_{18}}$	147.6 ± 0.68	2.49	2.54	1.24	2.75	1.32	2.59	0.64	1.29

*Values are mean ± SEM ($n = 3$)

**MIC: Minimum inhibitory concentration (μM)

[a]*S. a: Staphylococcus aureus* NCIM 5021; [b]*S. a: Staphylococcus aureus* NCIM 5022;[c]*S. a: Methicillin resistant Staphylococcus aureus* ATCC 43,300 (MRSA); [d]*S. e: Staphylococcus epidermidis NCIM* 2493; [e]*M.t. a:Mycobacterium sp.* NCIM 2984; [f]*K. p: Klebsiella pneumoniae* NCIM 2706; [g]*P. a: Pseudomonas aeruginosa* NCIM 2036; [h]*E. c: Escherichia coli* NCIM 2065

C_{11} and C_{14}) displayed bactericidal activity (MBC/MIC, 2), while all other tested compounds showed bacteriostatic activity (MBC/MIC, 4). Except four compounds, i.e. C_2, C_9, C_{10} and C_{13} (MBC/MIC, 2), all other tested compounds showed bacteriostatic activity (MBC/MIC, 4–8) against *S. aureus* ATCC 43300. On the other hand, compounds C_3, C_4, C_6, C_7, C_{11} C_{12} and C_{14} displayed bactericidal activity against *S. epidermidis* NCIM 2493 (MBC/MIC, 2), while in other tested compounds MIC values are much higher than MBC against this strain. Compounds were observed to be more active against *Mycobacterium sp* NCIM 2984 as evident by the bactericidal activity (MBC/MIC, 2) of compounds $C_{4\text{-}9}$, C_{11}, C_{12}, C_{14} and $C_{15,}$ Whereas only three compounds C_9, C_{14} and C_{15} exhibited bactericidal activity (MBC/MIC, 2) against *P. aeruginosa* NCIM 2036. Against another Gram-negative bacteria *E. coli* NCIM 2065 five compounds (C_3, C_8, C_9, C_{14} and C_{17}) displayed bactericidal activity (MBC/MIC, 2), while other tested compounds showed bacteriostatic activity (MBC/MIC, 4).

Time-kill assay

Time-kill kinetics was performed against *S. aureus* NCIM 5021 for compounds C_9 (at test concentrations of 9.8 and 19.7 μM) and C_{14} (at test concentrations of 12.7 and 25.5 μM). Results are compared with ciprofloxacin tested at concentrations of 3.1 and 6.2 μM. The time-kill kinetics profile of C_9 against *S. aureus* NCIM 5021 at test concentration of 19.7 μM showed 2log10 and > 3log10 reduction in number of viable cells, respectively, after 10 and 12 h of exposure, indicating bactericidal activity against this strain. At 9.8 μM test concentration, also this compound displayed bactericidal activity against *S. aureus* NCIM 5021 with a 3log10 reduction in number of viable cells after 12-h exposure; however, the rate of killing was comparatively less compared to the test concentration 19.7 μM. C_{14} showed a similar killing rate as C_9 against *S. aureus* NCIM 5021 with a 3log10 reduction in viable cell count relative to the initial inoculums after 12-h exposure. As shown in Fig. 2a, b, compounds C_9 and C_{14} completely eliminated this strain after 24 h. At both test concentrations of 3.1 and 6.2 μM, ciprofloxacin exhibited 3log10 reduction in *S. aureus* NCIM 5021 viable cell count after 10 h of exposure. Time-kill assay was also performed for compound C_{13} against *S. aureus* ATCC 43300 (MRSA) at test concentrations of 7.5 and 15 μM. At both concentrations, compound C_{13} displayed bactericidal activity with a decrease of ≥ 3log10 in viable cell count after 12-h exposure. The killing rate of ciprofloxacin was faster

at both test concentrations of 47.9 and 95.9 µM against *S. aureus* ATCC 43300 with a 3log10 reduction of viable cell count after 10 h of exposure. The results indicate that all three tested compounds have time-dependent bactericidal activity.

Cytotoxicity and selective index

The selectivity index (SI) of test compounds was determined as the ratio of IC_{50} on VERO cells and MIC against bacteria. The higher SI ratio indicates theoretically more efficacy and would be safety of a compound during *in vivo* treatment for a given bacterial infection. Result of cytotoxic activity against VERO cell line indicated a low effect of compounds $C_{1\text{-}18}$ with IC_{50} values higher than 104 µM (Table 5). Compounds $C_{1\text{-}3}$, C_5 and $C_{8\text{-}16}$ are observed to be slightly less cytotoxic (IC_{50} ~ 176.2–351.6 µM). Among the tested compounds, C_4 showed maximum cytotoxic effect with an IC_{50} value of 104.4 µM and an SI value in the range 0.50–1.02 µM against all tested bacterial strains. Compound C_{14} also exhibited lower SI values of 0.96, 0.98 and 0.96 µM, respectively, against *Mycobacterium sp* NCIM 2984, *P. aeruginosa* NCIM 2036 and *E. coli* NCIM 2065. Compounds C_3 and C_{13} with low cytotoxic effect (IC_{50s}, 349.3 and 349.8 µM, respectively) displayed high SI against all three tested strains of *S. aureus*. Compound C_{13} also showed high SI against the tested strains of *S. epidermidis* (SI, 11.81), *K. pneumoniae* (SI, 12.90) and *E. coli* (SI, 11.39). Another compound, i.e. $C_{15,}$ with less cytotoxic effect (IC_{50s}, 351.6 µM) showed relatively high SI of 27.68 and 14.52, respectively, against tested strain of *S. epidermidis*. However, low SI (< 6.80) was observed for this compound against all other tested bacterial strains. On the other hand, compound C_{16} exhibited high SI in the range of 12.99–14.83 against *S. aureus* NCIM 5022, MRSA ATCC 43300, *S. epidermidis NCIM* 2493 and *K. pneumoniae* NCIM 2706.

Prediction of absorption, distribution, metabolism, excretion and toxicity (ADMET) properties

ADMET properties of chemical compounds play important roles in the design and development of drug. In the present study, ADMET properties of the synthesized compounds $C_{1\text{-}18}$ were computed by SwissADME and (http://www.swissadme.ch) and pkCSM (http://biosig.unimelb.edu.au/pkcsm/prediction) online tools. ADMET properties, principle descriptors including hERG inhibition potential, AMES toxicity, Lipinski number of violations and PAINS number of alerts were taken into account (Table 6) to evaluate the acceptability for rational drug design.

The predicted total polar surface area (TPSA) of $C_{1\text{-}18}$ ranges between 70.2 and 116 $Å^2$ and is well within the recommended range (7–200 $Å^2$) (Table 5). The human intestinal absorption is observed to be between 88.72 and 93.82% showing the favourable kinetic profile of these compounds. The predicted central nervous system (CNS) permeability of $C_{1\text{-}18}$ ranges between −1.332 and −2.802, indicating no CNS activity of these compounds (−2 inactive and + 2 active). In addition, the apparent Caco-2 cell permeability (a model for the gut-blood barrier) for $C_{1\text{-}18}$ is observed to be within the range 0.64–1.809 cm/sec (> 0.90 high Caco-2 cell permeability) indicating the fast non-active transport of compounds C_1 and $C_{3\text{-}18}$. The predicted AMES toxicity result indicates the non carcinogenic potential of compounds C_1, C_2, $C_{5\text{-}11}$, C_{14}, C_{17} and C_{18}. Further, compounds $C_{1\text{-}18}$ did not exhibit the blockage of human ether-a-go-go (HERG) K^+ channels indicating no cardiotoxic effect of these compounds. These compounds are observed to be the inhibitors of some of the cytochrome P450s. The predicted zero Pains alert (PA) (Baell and Holloway, 2010) of all synthesized compounds indicated the absence of PAN assay interference structure and hence safety of these compounds. Compounds $C_{1\text{-}18}$ also obeyed Lipinski's rule (Lipinski, 2000) of five with zero violation, indicating their drug-like character of these compounds.

Drug candidates ADMET properties have been recognized as an important reason for late-stage failure in drug development. Consensus predictions of ADMET parameters are well-known strategy to improve the putative results in drug design field. These parameters predicted by different methods allowed for a consensus view of a given property (Andrade et al. 2020; Daina et al. 2017; Moda and Andricopulo 2012). Based on these observations, we also used QikProp module (Schrödinger software suite 2019–2) to predict the ADMET profiles of compounds $C_{1\text{-}18}$ (Supplementary Table S2). The predicted central nervous system (CNS) activity ranges between −2–1 on a scale of −2 as inactive and + 2 as active, indicating no CNS activity of these compounds. Brain/blood partition coefficient QPlogBB (−0.03–0.39) also indicated that these compounds are CNS negative and cannot cross the blood–brain barrier. The total solvent-accessible surface area (SASA) (490.8–581.48 $Å^2$) and polar surface area (PSA) (45.48–92.87 $Å^2$) of these molecules are well within the recommended range. The octanol/water partition coefficient (QPlogPo/w) (2.07–4.25) and aqueous solubility as indicated by the QPlogS (−5.07–−5.89) indicated the favourable absorption and distribution of compounds $C_{1\text{-}18}$. Predicted apparent Caco-2 cell permeability (QPPCaco) of these compounds is within the range 318–3830 nm/sec, indicative of fast non-active transport of these molecules, and is easy to absorb. Predicted QPlogKhsa values (−0.193–0.557), indicative of binding of these compounds to human serum albumin, are well within the recommended range (−1.5–1.5). This further indicated the favourable pharmacokinetic profile of these compounds. All eighteen compounds $C_{1\text{-}18}$ exhibited predicted

Table 6 In silico ADME prediction of newly designed molecules $\mathbf{C_{1\text{-}18}}$

Comp	[a]TPSA	[b]$LogP_{o/w}$	[c]% Intes Abs. (human)	[d]Caco2 permeability	[e]CYP inhibitor1A2/2C19/2D6/3A4	[f]CNS perm	[g]accptHB/ [i]donorHB	[h]hERG inhibitor	[i]AMES toxicity	[j]Lipinski #violations	[k]PAINS #alerts
$\mathbf{C_1}$	70.23	3.44	90.79	1.809	Yes/Yes/No/No	− 1.423	3/2	No	No	0	0
$\mathbf{C_2}$	70.23	3.44	91.87	1.221	Yes/Yes/No/No	− 1.354	2/2	No	No	0	0
$\mathbf{C_3}$	116.0	2.95	89.73	0.64	Yes/Yes/No/No	− 1.779	4/3	No	Yes	0	0
$\mathbf{C_4}$	116.0	2.47	90.54	0.996	Yes/Yes/No/No	− 1.889	4/3	No	Yes	0	0
$\mathbf{C_5}$	70.2	4.10	88.79	1.258	Yes/Yes/No/No	− 1.332	2/2	No	No	0	0
$\mathbf{C_6}$	83.1	2.35	93.61	1.314	Yes/Yes/No/No	− 2.799	3/2	No	No	0	0
$\mathbf{C_7}$	83.1	2.34	93.82	1.305	Yes/Yes/No/No	− 2.802	3/2	No	No	0	0
$\mathbf{C_8}$	86.0	3.38	89.42	1.346	Yes/Yes/Yes/Yes	− 1.712	2/2	No	No	0	0
$\mathbf{C_9}$	70.2	3.75	91.02	1.247	Yes/Yes/No/No	− 1.345	2/2	No	No	0	0
$\mathbf{C_{10}}$	70.2	4.15	88.72	1.12	Yes/Yes/No/No	−1.336	2/2	No	No	0	0
$\mathbf{C_{11}}$	79.4	2.89	91.43	1.353	Yes/Yes/Yes/No	− 2.035	3/4	No	No	0	0
$\mathbf{C_{12}}$	79.4	3.10	92.53	1.331	Yes/Yes/Yes/Yes	− 1.892	3/3	No	Yes	0	0
$\mathbf{C_{13}}$	98.4	3.18	90.24	1.332	Yes/Yes/No/No	− 1.462	2/2	No	Yes	0	0
$\mathbf{C_{14}}$	83.1	3.40	91.23	1.401	Yes/Yes/Yes/Yes	− 1.75	3/2	No	No	0	0
$\mathbf{C_{15}}$	86.0	3.39	89.75	1.324	Yes/Yes/Yes/Yes	− 1.815	2/3	No	Yes	0	0
$\mathbf{C_{16}}$	96.5	2.83	92.10	1.433	Yes/Yes/Yes/Yes	− 1.952	4/2	No	Yes	0	0
$\mathbf{C_{17}}$	70.2	3.73	90.65	1.295	Yes/Yes/No/No	− 1.364	2/2	No	No	0	0
$\mathbf{C_{18}}$	70.2	3.41	91.91	1.241	Yes/Yes/No/No	− 1.345	2/2	No	No	0	0

[a]Topological polar surface area (TPSA); [b]Log10 of the coefficient for solvent partitioning between 1-octanol and water; [c]percent intestinal absorption in human; [d]Predicted apparent Caco-2 cell permeability in cm/sec; [e]Predicted in vitro selective inhibitors for P450-mediated metabolism; [f]Predicted CNS permeability; [g]Estimated number of hydrogen bonds that would be accepted/donated by the compound; [h]blockage of HERG K^+ channels; [i]Predicted toxicity of compounds by AMES test; [j]Number of violations of Lipinski's rule of five; [k]Pains assay interference structure

IC_{50} values in the range −4.12–−4.88 for the blockage of human ether-a-go-go (HERG) K^+ channels (QPlogHERG) indicating the safety of these molecules. In addition, predicted number of primary metabolites of compounds $C_{1\text{-}18}$ is between 1 and 2, which further indicated the safety of these compounds. All compounds obeyed Lipinski's rule of five with 0 violation. Further, the drug-likeness of compounds was also assessed according to Jorgensen's rule of three [38], and all compounds obeyed this rule with zero violation.

Conclusion

In the present work, we performed hydroxybenzotriazole (HOBt) and 1-(3-dimethylaminopropyl)-3-ethylcarbodiimide hydrochloride (EDCl)-mediated synthesis of new N'-(1,3-benzothiazol-2-yl)-substituted benzamides $C_{1\text{-}18}$. High yields (80–95%) were obtained under relatively milder reaction conditions using dimethylformamide as solvent. Compound C_1, C_2, C_4, C_{12} and C_{13} synthesized by the N-heterocyclic carbene (NHC) organocatalysed direct oxidative amidation (Premaletha et al. 2017) resulted in 61–93% yield. Compound C_{13} synthesized by the coupling of 2-aminobenzothiazole and thiophene-2-carbonyl chloride in toluene in the presence of triethylamine resulted in 29% yield (Sovic et al. 2015). This compound demonstrated.

prominent antiproliferative effect with GI_{50} (50% of maximal inhibition of cell proliferation) concentrations of 29, 22 and 16 μM against HCT 116 (colon carcinoma), H 460 (lung carcinoma) and MCF-7 (breast carcinoma) cell lines. All our synthesized compounds were purified by column chromatography and characterized by FT-IR, ^{1}H-NMR, ^{13}C-NMR and HRMS spectral data. In the ^{1}H-NMR spectra splitting patterns for the aromatic protons were observed to be in agreement with the substitution pattern of respective compounds. In the ^{13}C-NMR spectrum of synthesized compounds, the carbonyl carbon of benzamide, azomethine carbon of benzothiazole and aromatic SP^2-hybridized carbon signals appeared in the expected region. The MIC value of synthesized compounds $C_{1\text{-}18}$ was evaluated by broth microdilution method using Mueller Hinton medium. Tested compounds showed variable activity against the tested Gram-positive and Gram-negative bacterial strains. Compounds C_3, C_5, C_9, $C_{13\text{-}15}$ and C_{17} exhibited significant activity against *S. aureus* NCIM 5021 with MIC values in the range 19.7–30.3 μM. Among all tested compounds, C_{13} possessing thiophene ring attached to the benzothiazole moiety via amide linkage exhibited maximum activity against *S. aureus* NCIM 5022 with MIC of 13.0 μM. Compound C_{13} also showed maximum activity against *S. aureus* ATCC 43300 with MIC of 15.0 μM compared to the standard drugs ciprofloxacin (MIC 86.4 μM) and gentamycin (MIC, 41.2 μM). This compound showed bactericidal activity against *S. aureus* ATCC 43300 in MBC determination and also eliminated this strain after 24 h. From the above results, it is evident that chemical structure of compound $\mathbf{C_{13}}$ may be utilized for further development of potent antibacterial and antiproliferative agents. Computed ADMET properties showed favourable pharmacokinetic profile of synthesized compounds $C_{1\text{-}18}$.

Supplementary Information The online version contains supplementary material available at https://doi.org/10.1007/s11696-021-01730-8.

Acknowledgements One of the authors would like to thank All India Council for Technical Education (AICTE) Quality Improvement Programme for providing fellowship.

Declarations

Conflict of interest On behalf of all authors, the corresponding author states that there is no conflict of interest.

References

Alanine A, Flohr A, Miller AK, Norcross RD, Riemer C (2001) Benzothiazole derivatives. WO2001097786A2, 27 Dec; Application No. PCT/EP01/06506, 8 June, 2001.

Amnerkar ND, Bhusari KP (2011) Synthesis of some thiazolyl aminobenzothiazole derivatives as potential antibacterial, antifungal and anthelmintic agents. J Enzyme Inhib Med Chem 26:22–28. https://doi.org/10.3109/14756360903555258

Andrade MM, Martins LC, Marques GV, Silva CA, Faria G, Caldas S, Dos Santos JS, Leclercq SY, Maltarollo VG, Ferreira RS, Oliveira RB (2020) Synthesis of quinoline derivatives as potential cysteine protease inhibitors. Future Med Chem 12:571–581. https://doi.org/10.4155/fmc-2019-0201

Azam MA, Suresh B (2012) Biological activities of 2-mercaptobenzothiazole derivatives: a review. Sci Pharm 80:789–823. https://doi.org/10.3797/scipharm.1204-1027

Baell JB, Holloway GA (2010) New substructure filters for removal of pan assay interference compounds (PAINS) from screening libraries and for their exclusion in bioassays. J Med Chem 53:2719–2740. https://doi.org/10.1021/jm901137j

Bailey TR, Pevear DC (2004) Benzothiazole compounds, compositions and methods for treatment and prophylaxis of rotavirus infections and associated diseases. WO2004078115A2, 16 Sep; Application No. PCT/US2004/005471, 25 Feb 2004.

Berkin KE, Kerr JW (1982) Tiaramide-a new oral drug for the treatment of asthma. Br J Clin Pharmacol 14:505–508. https://doi.org/10.1111/j.1365-2125.1982.tb02020.x

Bhat M, Belagali SL, Hemanth Kumar NK, Mahadevakumar S (2017) Synthesis and characterization of novel benzothiazole amide derivatives and screening as possible antimitotic and antimicrobial agents. Res Chem Intermed 43:361–378. https://doi.org/10.1007/s11164-016-2627-3

Bradshaw TD, Westwell AD (2004) The development of the antitumour benzothiazole prodrug, phortress, as a clinical candidate. Curr Med Chem 11:1009–1021. https://doi.org/10.2174/0929867043455530

Cai J, Sun M, Wu X, Chen J, Wang P, Zong X, Ji M (2013) Design and synthesis of novel 4-benzothiazole amino quinazolines Dasatinib derivatives as potential anti-tumor agents. Eur J Med Chem 63:702–712. https://doi.org/10.1016/j.ejmech.2013.03.013

Castanheiro T, Suffert J, Gulea M, Donnard M (2016) Aerobic copper-mediated domino three-component approach to 2-aminobenzothiazole derivatives. Org Lett 18:2588–2591. https://doi.org/10.1021/acs.orglett.6b00967

Catalano A, Carocci A, Defrenza I, Muraglia M, Carrieri A, Van Bambeke F, Rosato A, Corbo F, Franchini C (2013) 2-Aminobenzothiazole derivatives: search for new antifungal agents. Eur J Med Chem 64:357–364. https://doi.org/10.1016/j.ejmech.2013.03.064

Cindric M, Peric M, Kralj M, Martin-Kleiner I, David-Cordonnier MH, Paljetak HC, Matijasic M, Verbanac D, Karminski-Zamola G, Hranjec M (2018) Antibacterial and antiproliferative activity of novel 2-benzimidazolyl- and 2-benzothiazolyl-substituted benzo[b]thieno-2-carboxamides. Mol Divers 22:637–646. https://doi.org/10.1007/s11030-018-9822-7

Clinical and Laboratory Standard Institute (CLSI) (2007) Methods for dilution antibacterial susceptibility test for bacteria that grow aerobically, 7th ed. Approved Standard (MA7-A7), Clinical and Laboratory Standard Institute: Wayne, 27, pp. 13.

Dahl R, Lee AY, Kho C, Hajjar RJ (2015) Benzothiazole or benzoxazole compounds as sumo activators. WO2014036242 A3, July 7, 2015. Publication No. PCT/US2013/057264, Aug' 29, 2013.

Daina A, Michielin O, Zoete V (2017) SwissADME: a free web tool to evaluate pharmacokinetics, drug-likeness and medicinal chemistry friendliness of small molecules. Sci Rep 7:1–13. https://doi.org/10.1038/srep42717

Delmas F, Di Giorgio C, Robin M, Azas N, Gasquet M, Detang C, Costa M, Timon-David P, Galy JP (2002) In vitro activities of position 2 substitution-bearing 6-nitro- and 6-amino-benzothiazoles and their corresponding anthranilic acid derivatives against *Leishmania infantum and Trichomonas vaginalis*. Antimicrob Agents Chemother 46:2588–2594. https://doi.org/10.1128/AAC.46.8.2588-2594.2002

Franzblau SG, DeGroote MA, Cho SH, Andries K, Nuermberger E, Orme IM, Mdluli K, Angulo-Barturen I, Dick T, Dartois V, Lenaerts AJ (2012) Comprehensive analysis of methods used for the evaluation of compounds against *Mycobacterium tuberculosis*. Tuberculosis (edinb) 92:453–488. https://doi.org/10.1016/j.tube.2012.07.003

Gontijo VS, Viegas FPD, Ortiz CJC, de Freitas SM, Damasio CM, Rosa MC, Campos TG, Couto DS, Tranches Dias KS, Viegas C (2020) Molecular hybridization as a tool in the design of multitarget directed drug candidates for neurodegenerative diseases. Curr Neuropharmacol 18:348–407. https://doi.org/10.2174/1385272823666191021124443

Graham J, Wong CE, Day J, McFaddin E, Ochsner U, Hoang T, Young CL, Ribble W, DeGroote MA, Jarvis T, Sun X (2018) Discovery of benzothiazole amides as potent antimycobacterial agents. Bioorg Med Chem Lett 28:3177–3181. https://doi.org/10.1016/j.bmcl.2018.08.026

Greenberg A (2000) The amide linkage: Structural significance in chemistry, biochemistry, and materials science. John Wiley & Sons; 2000.

De Groote MA, Li W, Jackson M, Gonzalez-Juarrero M, Jarvis TC, Wong C, Graham J, Hoang T, Young CL, Ribble W, Day J, Li W, Jackson M, Gonzalez-Juarrero M, Sun X, Ochsner UA (2018) Optimization and lead selection of benzothiazole amide analogs toward a novel antimycobacterial agent. Front Microbiol 9:2231. https://doi.org/10.3389/fmicb.2018.02231

Hazra K, Nargund LVG, Rashmi P, Narendra Sharath Chandra JN, Nandha B, Harish MS (2012) Synthesis and comparative study of anti-mycobacterium activity of a novel series of fluoronitrobenzothiazolopyrazoline regioisomers. Arch Pharm Chem Life Sci 345:137–146. https://doi.org/10.1002/ardp.201100072

Heck RW, Tanhauser SM, Manda R, Tu C, Laipis PJ, Silverman DN (1994) Catalytic properties of mouse carbonic anhydrase V. J Biol Chem 269:24742–24746

Kerwin S, Hurley LH, De Luca MR, Moore BM (1997) Compounds and methods for providing pharmacologically active preparations and uses thereof. WO9748694A1, 24 Dec; Application No. PCT/US97/10643, 20 June 1997.

Klunk WE, Mathis CA, Wang Y (2014) Benzothiazole derivative compounds, compositions and uses. US Patent 8,691,185B2, 8 April; Application No. US 13/548014, July 12, 2012

Kim SG, Jung SL, Lee GH, Gong YD (2013) Novel solid-phase parallel synthesis of n-substituted-2-aminobenzo [d]thiazole derivatives via cyclization reactions of 2-iodophenyl thiourea intermediate resin. ACS Comb Sci 15:29–40. https://doi.org/10.1021/co300112b

Laursen LC, Lindqvist A, Hepburn T, Lloyd J, Perrett J, Sanders N, Rocchiccioli K (2003) The role of the novel D2/beta2-agonist, Viozan (sibenadet HCl), in the treatment of symptoms of chronic obstructive pulmonary disease: results of a large-scale clinical investigation. Respir Med 97:S23–S33. https://doi.org/10.1016/S0954-6111(03)80012-4

Levison ME (2004) Pharmacodynamics of antimicrobial drugs. Infect Dis Clin N Am 18:451–465. https://doi.org/10.1016/j.idc.2004.04.012

Lipinski CA (2000) Drug-like properties and the causes of poor solubility and poor permeability. J Pharmacol Toxicol Methods 44:235–249. https://doi.org/10.1016/S1056-8719(00)00107-6

Liu DC, Zhang HJ, Jin CM, Quan ZS (2016) Synthesis and biological evaluation of novel benzothiazole derivatives as potential anticonvulsant agents. Molecules 21:164. https://doi.org/10.3390/molecules21030164

Makhaeva GF, Kovaleva NV, Rudakova EV, Boltneva NP, Lushchekina SV, Faingold II, Poletaeva DA, Soldatova YV, Kotelnikova RA, Serkov IV, Ustinov AK, Proshin AN, Radchenko EV, Palyulin VA, Richardson RJ (2020) New multifunctional agents based on conjugates of 4-amino-2,3-polymethylenequinoline and butylated hydroxytoluene for alzheimer's disease treatment. Molecules 25:5891. https://doi.org/10.3390/molecules25245891

Mariappan G, Prabhat P, Sutharson L, Banerjee J, Patangia U, Nath S (2012) Synthesis and antidiabetic evaluation of benzothiazole derivatives. J Korean Chem Soc 56:251–256. https://doi.org/10.5012/jkcs.2012.56.2.251

Meltzer-Mats E, Babai-Shani G, Pasternak L, Uritsky N, Getter T, Viskind O, Eckel J, Cerasi E, Senderowitz H, Sasson S, Gruzman A (2013) Synthesis and mechanism of hypoglycemic activity of benzothiazole derivatives. J Med Chem 56:5335–5350. https://doi.org/10.1021/jm4001488

Mierau J, Schneider FJ, Ensinger HA, Chio CL, Lajiness ME, Huff RM (1995) Pramipexole binding and activation of cloned and expressed dopamine D2, D3 and D4 receptors. Eur J Pharmacol 290:29–36. https://doi.org/10.1016/0922-4106/90013-6

Moda TL, Andricopulo AD (2012) Consensus hologram QSAR modeling for the prediction of human intestinal absorption. Bioorg Med Chem Lett 22:2889–2893. https://doi.org/10.1016/j.bmcl.2012.02.061

Pankey GA, Sabath LD (2004) Clinical relevance of bacteriostatic versus bactericidal mechanisms of action in the treatment of gram-positive bacterial infections. Clin Infect Dis 38:864–870. https://doi.org/10.1086/381972

Parlati F, Ramesh UV, Singh Rajinder P, Donald G, Lowe R, Look GC (2005) Benzothiazole and thiazole[5,5-b] pyridine compositions and their use as ubiquitin ligase inhibitors. WO2005037845A1, 28 April; Application No. PCT/US2004/034397, 18 Oct, 2004.

Patel RV, Patel PK, Kumari P, Rajani DP, Chikhalia KH (2012) Synthesis of benzimidazolyl-1,3,4-oxadiazol-2ylthio-N-phenyl (benzothiazolyl) acetamides as antibacterial, antifungal and antituberculosis agents. Eur J Med Chem 53:41–51. https://doi.org/10.1016/j.ejmech.2012.03.033

Premaletha S, Ghosh A, Joseph S, Yetra SR, Biju AT (2017) Facile synthesis of N-acyl 2-aminobenzothiazoles by NHC-catalyzed direct oxidative amidation of aldehydes. Chem Commun 53:1478–1481. https://doi.org/10.1039/C6CC08640C

Santos AS, Silva AMS, Marques MMB (2020) Sustainable amidation reactions – recent advances. Eur J Org Chem 2020:2502–2516. https://doi.org/10.1002/ejoc.202000106

Saraswat P, Jeyabalan G, Hassan MZ, Ahsan MJ (2018) Design, synthesis and biological evaluation of benzothiazole-thiophene hybrids: a new class of potent antimicrobial agents. Anti-Infect Agents 16:57–63. https://doi.org/10.2174/2211352515666171124155327

Sashidhara KV, Avula SR, Doharey PK, Singh LR, Balaramnavar VM, Gupta J, Misra-Bhattacherya S, Rathaur S, Saxena AK, Saxena JK (2015) Designing, synthesis of selective and high-affinity chalcone-benzothiazole hybrids as Brugiamalayithymidylate kinase inhibitors: *in vitro* validation and docking studies. Eur J Med Chem 103:418–428. https://doi.org/10.1016/j.ejmech.2015.09.004

Sever B, Altıntop MD, Ozdemir A, Tabanca N, Estep AS, Becnel JJ, Bloomquist JR (2019) Biological evaluation of a series of benzothiazole derivatives as mosquitocidal agents. Open Chem 17:288–294. https://doi.org/10.1515/chem-2019-0027

Shaik B, Selam M, Tamminana R, Kammela PR (2019) Copper promoted C–S and C–N cross-coupling reactions: the synthesis of 2-(N-Aryolamino)benzothiazoles and 2-(N-Aryolamino)benzimidazoles. Tetrahedron 75:3865–3874. https://doi.org/10.1016/J.TET.2019.05.006

Sovic I, Viskic M, Bertosa B, Ester K, Kralj M, Hranjec M, Karminski-Zamola G (2015) Exploring antiproliferative activity of heteroaromatic amides and their fused derivatives using 3D-QSAR, synthesis, and biological tests. Monatsh Chem 146:1503–1517. https://doi.org/10.1007/s00706-015-1478-8

Srivastava SD, Sen JP (2008) Synthesis and biological evaluation of 2-aminobenzothiazole derivatives. Indian J Chem SecB 47B:1583–1586

Sutton JC, Wiesmann M, Wang W, Lindvall M, Lan J, Ramurthy S, Sharma A, Mieuli EJ, Klivansky LM, Lenahan WP, Kaufman S, Yang, H, Ng SC, Pfister K, Wagman A, Sung V, Sendzik M. (2009) 6-O-substituted benzoxazole and benzothiazole compounds and methods of inhibiting CSF-1R signalling. US Patent 7,553,854 B2, June 30; Application No. US11/737069, April 18, 2007.

Svendsen JS, Stensen W, Porter RA (2021) Benzothiazole derivatives as DYRK1 inhibitors. US Patent 1,092,7106 B2, Feb 23, 2021; Application No. 16/341630, Oct' 12, 2017

Ugwu DI, Okoro UC, Ukoha PO, Gupta A, Okafor SN (2018) Novel anti-inflammatory and analgesic agents: synthesis, molecular docking and *in vivo* studies. J Enzyme Inhib Med Chem 33:405–415. https://doi.org/10.1080/14756366.2018.1426573

Wang G, Fu Z, Huang W (2017) Access to amide from aldimine via aerobic oxidative carbene catalysis and LiCl as cooperative lewis acid. Org Lett 19:3362–3365. https://doi.org/10.1021/acs.orglett.7b01195

Wynne GM, Wren SP, Johnson PD, Price PD, De Moor O, Nugent G, Storer R, Pye RJ, Dorgan CR (2009) Preparation of benzoxazoles, benzimidazoles, benzothiazoles, indoles and their analogs for the treatment of muscular dystrophy and cachexia. WO2009019504A1, 12 Feb; Applcation No. PCT/GB2008/050648, 1 Aug, 2008.

Xie Y, Deng S, Chen Z, Yan S, Landry DW (2006) Identification of small-molecule inhibitors of the Abeta-ABAD interaction. Bioorg Med Chem Lett 16:4657–4660. https://doi.org/10.1016/j.bmcl.2006.05.099

Yoshida M, Hayakawa I, Hayashi N, Agatsuma T, Oda Y, Tanzawa F, Iwasaki S, Koyama K, Furukawa H, Kurakatad S, Suganob Y (2005) Synthesis and biological evaluation of benzothiazole derivatives as potent antitumor agents. Bioorg Med Chem Lett 15:3328–3332. https://doi.org/10.1016/j.bmcl.2005.05.077

Zoccolella S, Beghi E, Palagano G, Fraddosio A, Guerra V, Samarelli V, Lepore V, Simone IL, Lamberti P, Serlenga L, Logroscino G (2007) Riluzole and amyotrophic lateral sclerosis survival: a population-based study in southern Italy. Eur J Neurol 14:262–268. https://doi.org/10.1111/j.1468-1331.2006.01575.x